BIOCHEMISTRY
including biophysical chemistry & molecular biology

Article

pubs.acs.org/biochemistry

Differential Localization of G Protein $\beta\gamma$ Subunits

Katherine M. Betke,[†] Kristie L. Rose,[‡] David B. Friedman,[‡] Anthony J. Baucum, II,[§,⊥] Karren Hyde,[†] Kevin L. Schey,[‡,∥] and Heidi E. Hamm*[,†]

[†]Department of Pharmacology, [‡]Mass Spectrometry Research Center, [§]Department of Molecular Physiology and Biophysics, and [∥]Department of Biochemistry, Vanderbilt University Medical Center, Nashville, Tennessee 37232-6600, United States

[⊥]Department of Biology, Indiana University-Purdue University Indianapolis, Indianapolis, Indiana 46202, United States

Supporting Information

ABSTRACT: G protein $\beta\gamma$ subunits play essential roles in regulating cellular signaling cascades, yet little is known about their distribution in tissues or their subcellular localization. While previous studies have suggested specific isoforms may exhibit a wide range of distributions throughout the central nervous system, a thorough investigation of the expression patterns of both Gβ and Gγ isoforms within subcellular fractions has not been conducted. To address this, we applied a targeted proteomics approach known as multiple-reaction monitoring to analyze localization patterns of Gβ and Gγ isoforms in pre- and postsynaptic fractions isolated from cortex, cerebellum, hippocampus, and striatum. Particular Gβ and Gγ subunits were found to exhibit distinct regional and subcellular localization patterns throughout the brain. Significant differences in subcellular localization between pre- and postsynaptic fractions were observed within the striatum for most Gβ and Gγ isoforms, while others exhibited completely unique expression patterns in all four brain regions examined. Such differences are a prerequisite for understanding roles of individual subunits in regulating specific signaling pathways throughout the central nervous system.

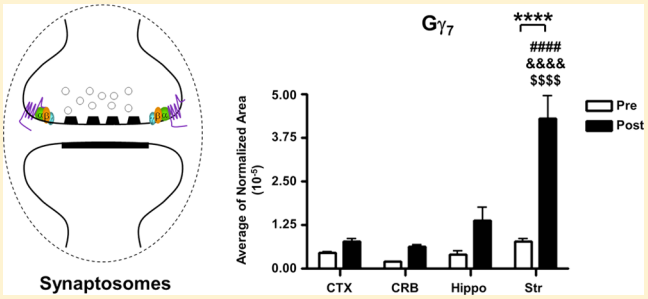

Heterotrimeric G proteins play essential roles in cellular communication by transducing extracellular signals from G protein-coupled receptors (GPCRs) to a wide range of downstream effectors. The fidelity of this process depends in part upon the G protein itself, as it requires guanine nucleotide-binding α subunits to exchange GDP for GTP and reversibly dissociate from $\beta\gamma$ dimers before each can interact with effectors.[1] Originally, signaling was thought to be mediated solely through Gα subunits;[2] however, G$\beta\gamma$ complexes are now widely recognized as independent signaling molecules, with effectors such as adenylyl cyclase, phospholipase C-β, PI 3-kinase, and components of the mitogen-activated protein kinase cascade.[3−8] Additional effectors such as voltage-gated calcium and potassium channels, as well as members of the exocytotic machinery, regulate membrane voltage and neurotransmitter release.[9−17] With such diversity, it is hardly surprising that G$\beta\gamma$ subunits make up a strongly expressed, structurally diverse family, with 5 and 12 genes encoding 5 β and 12 γ protein subunits, respectively.[18,19] Historically, specificity has largely been attributed to the α subunits as only modest functional differences were observed in the ability of $\beta\gamma$ isoform combinations to regulate effectors *in vitro*.[20,21] More recent evidence indicates this may not be the case in intact cells, however, as studies have suggested very specific roles for Gβ and Gγ isoforms.[22−27] However, while specific receptors and effectors may utilize unique complements of G protein α, β, and γ subunits, we have little understanding of which G protein heterotrimers exist *in vivo*, the factors controlling their distribution in tissues, their subcellular expression, or their functional relevance in the context of the whole organism. To this end, a greater understanding of the tissue localization and subcellular distribution of G$\beta\gamma$ isoforms will be of particular importance in determining which of the many possible combinations are likely to occur physiologically, what roles each may play in regulating signaling cascades, and their impact in disease.

The majority of G protein β and γ subunits have been detected in the central nervous system (CNS).[28−34] Our understanding of their distributions largely stems from *in situ* hybridization studies; specifically, RNAs from some β and γ isoforms exhibit wide distributions, while others show expression more restricted to specific brain regions and cell types, possibly reflecting unique functions.[35−40] Although a few studies have examined protein expression,[36,39−42] efforts at this level have been less reliable as the high level of sequence identity between isoforms has limited the development of reliable subunit specific reagents.[43] Proteomic analysis offers a powerful way to deepen our understanding of the regional and subcellular localization patterns of G$\beta\gamma$ isoforms as they can be undertaken using endogenous tissue without the need for isoform specific antibodies. Studies examining synaptic

Received: January 21, 2014
Revised: February 24, 2014
Published: February 25, 2014

   dx.doi.org/10.1021/bi500091p | *Biochemistry* 2014, 53, 2329−2343

proteomes to date have largely focused on analyzing the global expression of proteins involved in synaptic functions,[44−52] and no study has yet sought to specifically examine G protein localization patterns. As a result, while a few β and γ isoforms have been identified or even localized to subcellular fractions in discovery-based experiments,[53−57] the majority have yet to be described. Such studies demonstrate that even at isolated nerve endings, cells express large numbers of proteins, making identification of all of the proteins in a sample problematic. Further, highly abundant proteins may mask those expressed at lower levels. To overcome these problems, we applied a targeted proteomics approach known as multiple-reaction monitoring (MRM),[58,59] which allowed us to accurately identify unique G protein isoforms in complex mixtures. Using this approach, we analyzed regional and subcellular localization patterns of Gβ and Gγ isoforms in different brain regions. Interestingly, we found that these subunits exhibit distinct regional and subcellular localization patterns throughout the CNS, suggesting roles for individual subunits in regulating specific signaling pathways.

MATERIALS AND METHODS

Protein Standards. $G\beta_1\gamma_1$ was purified from bovine retina as described previously.[60] Recombinant $G\beta_1\gamma_2$ and $G\beta_5\gamma_2$ were expressed in Sf9 cells and purified via a His_6-tagged $G\gamma_2$ using nickel-nitrilotriacetic acid affinity chromatography (Sigma-Aldrich, St. Louis, MO). Human Gγ subunit cDNAs for $G\gamma_4$, $G\gamma_5$, $G\gamma_7$, $G\gamma_{11}$, and $G\gamma_{13}$ were subcloned by polymerase chain reaction from pcDNA3.1+ clones (Missouri S&T cDNA Resource Center) into pGEX-6p-1 (GE Healthcare). The sequences of the resultant vectors, hGgamma($_x$).pGEX-6p-1, were verified, and GST fusion proteins were expressed in Rosetta Competent Cells (EMD Millipore). After induction with 1 mM IPTG followed by a 4 h incubation at 37 °C, the resultant Gγ proteins were batch purified using Glutathione Sepahrose 4 Fast Flow (GE Healthcare) and eluted with 10 mM reduced free acid glutathione (Calbiochem).

Animals. Adult, male C57Bl6/J mice were decapitated, and the cortex, cerebellum, neostriatum (termed the striatum), and hippocampus were dissected, frozen on dry ice, and stored at −80 °C until they were processed. To minimize post-mortem differences, all brain regions were dissected at the same time and processed in parallel. All animal protocols were conducted in accordance with the recommendations in the Guide for the Care and Use of Laboratory Animals of the National Institutes of Health and were approved by the Vanderbilt Institutional Animal Care and Use Committee.

Antibodies. The following primary antibodies were used for immunoblotting (dilutions indicated): rabbit anti-Gβ (Santa Cruz, catalog no. sc-378, 1:15000), mouse anti-*N*-methyl-D-aspartate receptor-1 (NMDAR1) (BD Pharmingen, catalog no. 556308, 1:2000), mouse anti-postsynaptic density-95 (PSD-95) (Neuromab, catalog no. 75-028, 1:20000), mouse anti-glyceraldehyde-3-phosphate dehydrogenase (GAPDH) (Millipore, catalog no. MAB374, 1:20000), and mouse anti-syntaxin-1 (Santa Cruz, catalog no. sc-12736, 1:2000). Horseradish peroxidase-conjugated secondary antibodies were obtained from Perkin-Elmer and used at the following dilutions: goat anti-rabbit (1:20000) and goat anti-mouse (1:10000 for NMDAR1 and syntaxin and 1:20000 for PDS-95 and GAPDH).

Synaptosome Preparation and Subcellular Fractionation. Subcellular fractions were prepared as previously described.[61] Briefly, four whole mouse cortex (CTX), cerebellum (CRB), striatum (Str), or hippocampus (Hippo) samples were pooled and homogenized in 10 mL of a 0.32 M sucrose solution [0.32 M sucrose, 4.2 mM potassium 4-(2-hydroxyethyl)-1-piperazineethanesulfonate (HEPES) (pH 7.4), 0.1 mM $CaCl_2$, 1 mM $MgCl_2$, 1.54 μM aprotinin, 10.7 μM leupeptin, 0.95 μM pepstatin, and 200 μM phenylmethanesulfonyl fluoride (PMSF)]. Homogenates were centrifuged at 1000*g* and 4 °C for 10 min to pellet nuclei and membrane debris before supernatants were transferred to clean conical tubes. Pellets were resuspended in 10 mL of 0.32 M sucrose; the centrifugation step was repeated, and supernatants were combined. Following mixing, supernatants were centrifuged at 10000*g* and 4 °C for 20 min to produce crude synaptosome preparations. Supernatants were discarded and pellets gently resuspended in 4 mL of hypotonic lysis buffer [20 mM Tris (pH 6.0), 0.1 mM $CaCl_2$, 1 mM $MgCl_2$, 1% Triton X-100, 1.54 μM aprotinin, 10.7 μM leupeptin, 0.95 μM pepstatin, and 200 μM PMSF] before being incubated on ice for 20 min to lyse membranes. Lysates were cleared via ultracentrifugation at 100000*g* and 4 °C for 2 h in a SW-55 Ti rotor (Beckman Coulter) and supernatants (consisting of the "perisynaptic/cytosolic" fraction) transferred to clean conical tubes. Pellets were resuspended in 1 mL of Tris buffer [20 mM Tris (pH 8.0), 1% Triton X-100, 1.54 μM aprotinin, 10.7 μM leupeptin, 0.95 μM pepstatin, and 200 μM PMSF] and incubated on ice for 20 min. Lysates were centrifuged at 10000*g* and 4 °C for 30 min and supernatants containing enriched presynaptic fractions collected. Finally, pellets were resuspended in 200 μL of a 1× phosphate-buffered saline/1% SDS mixture and centrifuged at 10000*g* and 4 °C for 30 min. Supernatants containing enriched postsynaptic fractions were collected. Protein concentrations were determined with a BCA assay kit (Pierce).

Immunoblot Analysis. To examine the enrichment of pre- and postsynaptic fractions, Western blot analysis was performed; 7 μg of each fraction was diluted in 4× sodium dodecyl sulfate−polyacrylamide gel electrophoresis (SDS−PAGE) sample buffer containing 100 mM dithiothreitol, heated for 5 min at 70 °C, and resolved on 10 or 15% SDS−PAGE gels. Proteins were transferred electrophoretically to a nitrocellulose membrane in cold transfer buffer consisting of 200 mL of 3-(cyclohexylamino)-1-propanonesulfonic acid (CAPS), 200 mL of methanol, and 1600 mL of water. Following transfer, membranes were stained with Ponceau and cut between appropriate molecular weight markers. Membranes were blocked with slight agitation for 1 h in a buffer of Tris-buffered saline (TBS) with 5% milk and 0.1% Tween 20 (Sigma-Aldrich). Membranes were then washed five times for 5 min in TBS with 0.1% Tween 20 on a shaker before being incubated with the appropriate primary antibodies in TBS with 5% milk and 0.2% Tween 20 on a shaker table at 4 °C overnight. The next day, membranes underwent five 5 min washes on a shaker table in TBS with 0.1% Tween 20 before the appropriate secondary antibodies were diluted into TBS with 5% milk and 0.2% Tween 20 followed by gentle agitation on a shaker with the membranes for 1 h at room temperature. Finally, membranes were washed three times for 10 min in TBS with 0.1% Tween 20 followed by two 15 min washes in TBS. Immunoblots were developed using Western Lightning Chemiluminescence Reagent Plus (NEL104) from Perkin-Elmer as per their published protocols. Imaging was conducted using a Bio-Rad imager.

Development and Validation of Targeted Mass Spectrometry Methods. Purified G$\beta\gamma$ isoforms or enriched protein pre- and postsynaptic fractions were separated by SDS−PAGE (15% acrylamide) and stained with colloidal Coomassie Blue (Invitrogen). Gel bands corresponding to the molecular weights of Gβ and Gγ subunits were excised, chopped into 1 mm^3 pieces, reduced with dithiothreitol, alkylated with iodoacetamide, and digested with trypsin. Individual G protein subunit digests from purified proteins were analyzed via nanoflow reverse phase liquid chromatography−tandem mass spectrometry (LC−MS/MS) on an LTQ-Orbitrap XL mass spectrometer (Thermo Scientific), while those from enriched protein synaptic fractions were analyzed on an LTQ-Orbitrap Velos mass spectrometer (Thermo Scientific). Peptides were loaded onto a capillary reverse phase analytical column (360 μm outside diameter × 100 μm inside diameter) using an Eksigent NanoLC high-performance liquid chromatography system and autosampler. The analytical column was packed with 20 cm of C18 reverse phase material (Jupiter, 3 μm beads, 300 Å, Phenomenex), equipped with a laser-pulled emitter tip. Peptides were gradient-eluted at a flow rate of 500 nL/min, and the mobile phase solvents consisted of 0.1% formic acid and 99.9% water (solvent A) and 0.1% formic acid and 99.9% acetonitrile (solvent B). A 45 min gradient was performed for purified G protein samples, consisting of the following: from 0 to 10 min, 2% B (during sample loading); from 10 to 28 min, 2 to 40% B; from 28 to 34 min, 40 to 90% B; from 34 to 35 min, 90% B; from 35 to 37 min, 90 to 2% B; from 37 to 45 min, 2% B (column equilibration). In comparison, a 90 min gradient was performed for G protein samples isolated from enriched protein presynaptic fractions consisting of the following: from 0 to 10 min, 2% B; from 10 to 50 min, 2 to 35% B; from 50 to 60 min, 35 to 90% B; from 60 to 65 min, 90% B; from 65 to 70 min, 90 to 2% B; from 70 to 90 min, 2% B. Upon gradient elution, peptides were mass analyzed on an LTQ Orbitrap XL or LTQ Orbitrap Velos mass spectrometer (Thermo Scientific). The instruments were operated using a data-dependent method with dynamic exclusion enabled. Full scan (m/z 300−2000) spectra were acquired with the Orbitrap as the mass analyzer (resolution of 60000), and the 5 most abundant (LTQ Orbitrap XL) or 16 most abundant ions (LTQ Orbitrap Velos) in each MS scan were selected for fragmentation via collision-induced dissociation (CID) in the LTQ. For selected LC−MS/MS analyses, the LTQ Orbitrap Velos was operated using a combination method of data-dependent and targeted scan events. Targets were of specific m/z values corresponding to unique Gβ or Gγ peptides selected from theoretical *in silico* digestions of the G protein subunits. Peptides were identified via database searching with Sequest[62] (Thermo Scientific). Tandem mass spectra were searched against *Bos taurus*, *Mus musculus*, or *Homo sapiens* subsets of the UniprotKB protein database (http://www.uniprot.org), and search results were assembled using Scaffold version 3.0 (Proteome Software). Although isoforms were purified from bovine retina, as well as cloned using human sequences, peptides unique to each G$\beta\gamma$ isoform being monitored were shown to be identical across all three species, allowing use of these proteins for assay development. All searches were configured to use variable modifications of carbamidomethylation on cysteine and oxidation of methionine. The selected peptides from each G protein β and γ subunit were validated via manual interrogation of the raw tandem mass spectra using QualBrowser software (Xcalibur version 2.1.0, Thermo Scientific), and as an additional validation criterion, the observed monoisotopic m/z value was required to be within 5 ppm of the theoretical m/z value for a given peptide. Identified peptides unique to G protein isoforms were selected, and their MS/MS spectra were examined to select precursor−product ion transitions for targeted MRM experiments. MRM methods were generated in Skyline[63] before being exported and employed for G protein-targeted experiments on a TSQ Vantage triple quadrupole mass spectrometer (Thermo Scientific). Unscheduled MRM runs were performed on purified G$\beta\gamma$ isoforms when available, as well as enriched pre- and postsynaptic fractions from mouse cortex, to evaluate intensities of precursor and product ions identified in early discovery proteomic runs. The resulting MRM data were imported and analyzed in Skyline. Extracted ion chromatographic peaks were manually interrogated and correct peaks chosen on the basis of retention times, how well the relative distribution of transition ions matched those from discovery experiments, and dot plot values. Dot plot values were calculated by comparison of transition ion intensities in MRM data relative to product ion intensities observed in tandem mass spectra acquired in LTQ-Orbitrap discovery experiments. Following validation, precursor and product ion lists were refined to include only the optimal precursor and transitions necessary to accurately identify each G protein isoform. Refined methods were required to include at least two distinct peptides for each G protein isoform, as well as three transitions for each peptide being monitored. These data and criteria were then used to generate scheduled MRM methods that could be applied to pre- and postsynaptic fractions from different brain regions.

Application of Targeted Proteomics Methods to Enriched Synaptic Fractions. Once refined, scheduled MRM methods were applied to in-gel-digested proteins from mouse brain-enriched pre- and postsynaptic fractions isolated from cortex, cerebellum, hippocampus, and striatum; 50 μg of total protein from each fraction was separated by SDS−PAGE for each brain region and digested as described. Gβ peptides were analyzed by a single 60 min scheduled MRM analysis, while Gγ peptides were split into two 60 min scheduled MRM runs. Biological samples were randomized to ensure any drift in assay performance would not affect subsets disproportionately. Briefly, utilizing a trap column setup, peptides were first loaded onto a 100 μm × 4 cm C18 reverse phase column, which was connected in line to a 20 cm × 100 μm (Jupiter, 3 μm, 300 Å) analytical column. Peptides were gradient-eluted into a TSQ-Vantage instrument (Thermo Scientific) using a nano-electrospray source. Peptides were resolved using an aqueous to organic gradient with a 60 min total cycle time. Scheduled instrument methods encompassing a 10 min window around the measured retention time along with calculated collision energies were created using Skyline. The Q1 peak width resolution was set to 0.7; the collision gas pressure was 1 mTorr, and a cycle time of 5 s was utilized. The resulting RAW instrument files were imported into Skyline for peak-picking and quantitation. Data analysis using Skyline was performed to assess enrichment of individual G protein subunits in pre- or postsynaptic fractions. Transition ion intensities were summed for each precursor, and these data were used to generate extracted ion chromatographic peaks of co-eluting transitions. As described previously, chromatographic peaks were manually interrogated and correct peaks chosen on the basis of retention times, dot plot values, and relative distributions of transition

Table 1. Internal Reference Peptides and MRM Transitions Added to All G Protein Samples

peptide sequence	precursor m/z	charge	collison energy	product ion m/z
SSAAPPPPPR	493.7683	+2	18	287.1728, 379.2327, 476.2855, 670.3910
TASEFDSAIAQDK	695.8324	+2	24	740.4028, 855.4298, 1002.4982, 1218.5728
ELGQSGVDTYLQTK	773.8956	+2	26	761.4286, 876.4553, 1032.5452, 1119.5772
LTILEELR	498.8018	+2	18	214.1306, 427.2539, 669.3805, 782.4646

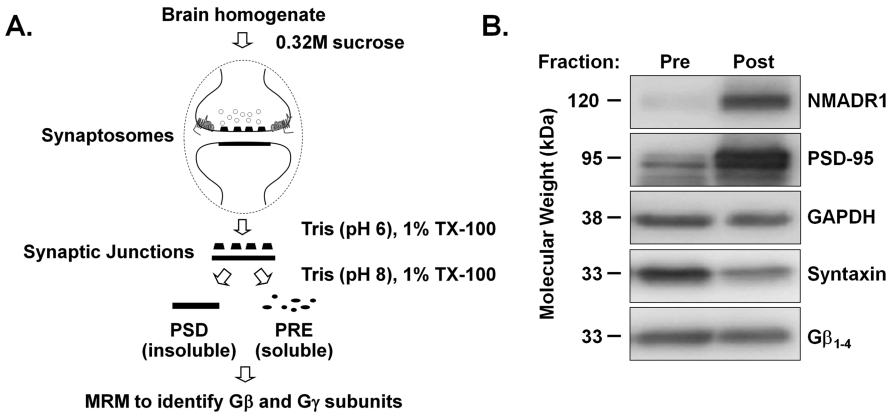

Figure 1. Distribution of marker proteins in pre- and postsynaptic fractions. (A) Experimental protocol for the isolation of synaptosomes from mouse brain tissue and the enrichment of pre- and postsynaptic fractions. (B) Representative immunoblots for NMDAR1, postsynaptic density 95 (PSD-95), GAPDH, syntaxin-1, and Gβ isolated from enriched pre- and postsynaptic fractions of adult mice.

ions. For peptides where a correct peak could confidently be chosen, a signal-to-noise (S/N) ratio of at least 30 was required to be included in analyses; those that did not meet this criterion were removed from further analyses. Four internal reference peptides, SSAAPPPPPR, TASEFDSAIAQDK, ELGQSGVDTYLQTK, and LTILEELR (Table 1), were used to evaluate drift in assay performance and to allow data to be normalized. Each reference peptide (5 fmol) was spiked into all samples and monitored throughout all MRM experiments. BSA controls were monitored at regular intervals between samples to evaluate instrument performance. The integrated area under the curve was calculated for all transitions. Coefficients of variation (CVs) were calculated for BSA controls and spiked in reference peptides using the relationship CV = (average total AUC)/(SD of total AUC), where AUC represents the integrated area under the curve for all transitions and SD represents the standard deviation of the total AUC. To allow comparison between experiments conducted on different days, the integrated area under the curve for each peptide was normalized relative to the internal reference peptide that was closest in retention time to it. This generated a normalized total area for each peptide.

A modified labeled reference peptide (LRP) method[64] was applied using the internal reference peptides described above to compare brain regions and subcellular fractions for each G protein isoform. To evaluate the expression of each G protein isoform using this method, a ratio between the normalized total area for each peptide being monitored and the total area for one internal reference peptide, ELGQSGVSTYLQTK, was calculated. The ratios for all peptides monitored for a given isoform were then averaged and the averages plotted for each protein. Fold differences were calculated to compare expression of each G protein isoform in pre- and postsynaptic fractions within a brain region as well as pre- or postsynaptic fractions between brain regions. To compare expression within a brain region, the average normalized total area calculated from the postsynaptic fraction was divided by the average normalized total area calculated from the presynaptic fraction of that same region (e.g., CTX post normalized total area/CTX pre normalized total area). To compare expression in presynaptic fractions of different brain regions, the average normalized total area from a presynaptic fraction in one brain area was divided by the average normalized total area from a presynaptic fraction from another brain region (e.g., CTX pre normalized total area/CRB pre normalized total area). This was also done for comparisons of postsynaptic fractions between brain regions.

Statistical Analysis. To evaluate data for comparison of brain regions and subcellular fractions, a two-way analysis of variance (ANOVA) was used to account for differences in isoform expression that could be due to their location in the CNS (i.e., CTX or CRB; termed brain region effect), their subcellular location (i.e., pre- or postsynaptic; termed the fraction effect), or a combination of the two (termed the interaction effect). To determine where specific differences in expression occurred, a Tukey post hoc test was used. In the case of Gβ_5, data were evaluated using an unpaired t test.

RESULTS

Synaptosome Subcellular Fractionation Efficiency. To assess the localization patterns of different G protein isoforms, we made use of a brain synaptosomal preparation and subcellular fractionation protocol that would allow us to reduce sample complexity (Figure 1A). Synaptosomes are a widely used preparation for studying synaptic biochemistry as they contain the complete presynaptic terminus, including mitochondria and synaptic vesicles, as well as the postsynaptic

dx.doi.org/10.1021/bi500091p | Biochemistry 2014, 53, 2329−2343

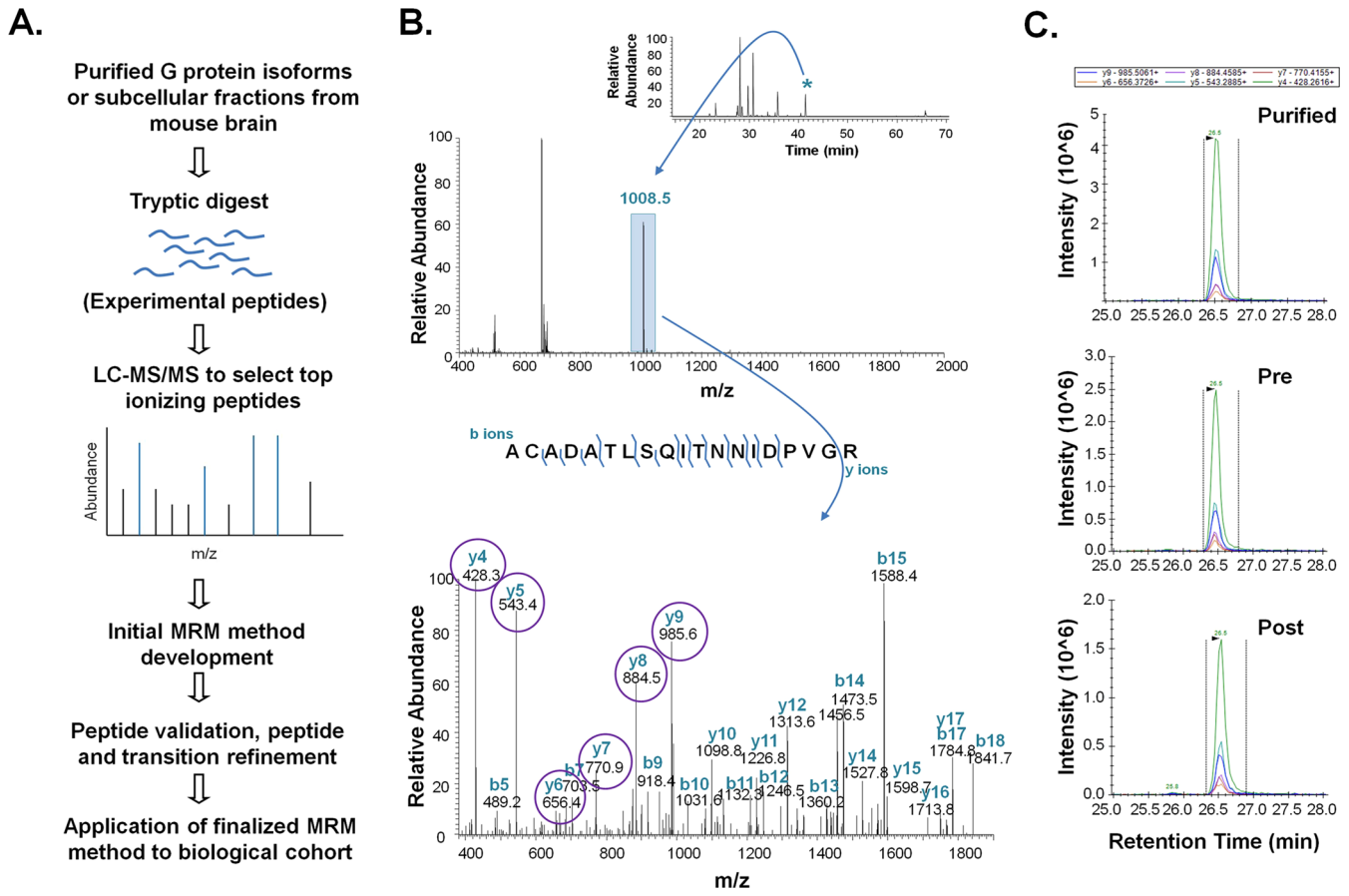

Figure 2. Development and validation of targeted mass spectrometry methods. (A) Workflow for the development and validation of multiple-reaction monitoring (MRM) methods. (B) LC−MS/MS identification of the Gβ_1 peptide, ACADATLSQITNNIDPVGR. The top panel shows the mass spectrum of peptides eluting at 42 min. The peak at m/z 1008.5 (blue) corresponds to the $[M + 2H]^{2+}$ precursor ion of the Gβ_1 peptide. The inset shows the base peak chromatogram; the asterisk denotes the peak of the peptide at 42 min. The bottom panel shows the MS/MS spectrum of the ion at m/z 1008.5. Observed b- and y-type product ions are labeled, and sites of amide bond cleavage are denoted with brackets. Circles indicate product ions imported into initial MRM methods for evaluation. (C) Chromatographic traces for each transition generated from fragmentation of the $[M + 2H]^{2+}$ precursor (m/z 1008.5) to its corresponding y product ions (y4−y9; different colors) during MRM. Transition peaks were readily observed following analysis of purified Gβ_1 (top), and equivalent transitions were evident upon analysis of pre- and postsynaptic fractions isolated from mouse brain cortical tissue (middle and bottom, respectively).

membrane and postsynaptic density (PSD).[44,53] To verify the efficiency of our fractionation protocol, we examined the enrichment of well-established synaptic markers in our pre- and postsynaptic fractions. Protein (7 μg of total protein) from each isolated fraction was separated on SDS−PAGE gels, electroblotted onto nitrocellulose membranes, and immunostained with antibodies against NMDAR1, PSD-95, GAPDH, syntaxin-1, and Gβ. Figure 1B reveals the high level of enrichment of NMDAR1 and PSD-95 in the postsynaptic fraction, whereas the presynaptic fraction is enriched with syntaxin-1. Although syntaxin-1 is thought to be primarily concentrated at the site of neurotransmitter release in neurons, it has also been shown to be expressed postsynaptically,[65] accounting for its presence in the postsynaptic fraction following enrichment in this study. Conversely, GAPDH, a cytosolic protein, shows equal levels of expression in both fractions, although the level of expression in pre- and postsynaptic fractions was lower than that seen in cytosolic fractions (data not shown). Similarly, Gβ was expressed equally in both pre- and postsynaptic factions using a pan-Gβ antibody (Figure 1B).

Development and Validation of Targeted Mass Spectrometry Methods. Target peptides and transitions for MRM studies were obtained by analyzing purified, recombinant G$\beta\gamma$ proteins (Gβ_1, Gβ_5, Gγ_2, Gγ_4, Gγ_5, Gγ_7, Gγ_{11}, and Gγ_{13}) when available, as well as enriched pre- and postsynaptic fractions from mouse cortex. Figure 2A illustrates a schematic of the workflow for targeted MRM development. *In silico* tryptic digests were initially performed and peptides that were unique to a single G protein isoform preselected. Peptides were then further screened for uniqueness by performing a protein basic local alignment search tool search. Only precursor peptides unique to a single G protein isoform and not found in protein sequences belonging to related or unrelated proteins were chosen (Table 2). Following tryptic digestion, extracted peptides from purified G protein samples were initially analyzed on an LTQ-Orbitrap XL mass spectrometer, while those from enriched pre- and postsynaptic fractions were analyzed on an LTQ-Orbitrap Velos mass spectrometer. Data-dependent LC−MS/MS runs identified >200 proteins in synaptic fractions from gel regions corresponding to the expected molecular weight of Gβ and Gγ subunits (data not shown). From these initial experiments, peptides corresponding to four of the five Gβ isoforms (Gβ_1, Gβ_2, Gβ_4, and Gβ_5) were identified and validated, as well as eight of the Gγ isoforms (Gγ_2, Gγ_3, Gγ_4, Gγ_5, Gγ_7, Gγ_{11}, Gγ_{12}, and Gγ_{13}). Unique peptides corresponding to Gβ_3, Gγ_8, and Gγ_{10} were not identified in subcellular

dx.doi.org/10.1021/bi500091p | *Biochemistry* 2014, 53, 2329−2343

Table 2. Precursor Peptides and MRM Transitions Used for the Identification of Gβ and Gγ Isoforms in Enriched Pre- and Postsynaptic Fractions[a]

G protein isoform	sequence position	peptide sequence	precursor m/z	charge	collison energy	product ion m/z
$G\beta_1$	24−42	(K)A**C**ADATLSQITNNIDPVGR(I)	1008.4944	+2	33	428.2616, 543.2885, 884.4585, 985.5061
	138−150	(R)ELAGHTGYLS**C**CR(F)	762.3401	+2	26	641.2768, 858.3597, 915.3811, 1016.4288
	198−209	(R)LFVSGA**C**DASAK(L)	613.2977	+2	21	483.2215, 779.3352, 866.3673, 965.4357
	284−301	(R)LLLAGYDDFN**C**NVWDALK(A)	1064.0144	+2	35	632.3402, 894.3883, 950.9304, 1119.5252
$G\beta_2$	24−42	(K)A**C**GDSTLTQITAGLDPVGR(I)	966.4782	+2	32	428.2616, 543.2885, 713.3941, 885.4789
		(K)A**C**GDSTLTQITAGLDPVGR(I)	644.6546	+3	27	428.2616, 543.2885, 713.3941, 885.4789
	198−209	(R)TFVSGA**C**DASIK(L)	628.3030	+2	22	504.2449, 821.3822, 908.4142, 1007.4826
	257−280	(R)ADQELLMYSHDNII**C**GITSVAFSR(S)	914.1072	+3	37	409.2194, 480.2565, 666.3570, 767.4046
		(R)ADQELL**M**YSHDNII**C**GITSVAFSR(S)	919.4388	+3	37	409.2194, 480.2565, 666.3570, 937.5102
$G\beta_4$	198−209	(R)TFVSGA**C**DASSK(L)	615.2770	+2	21	491.2189, 667.2716, 795.3301, 882.3622, 981.4306
	305−314	(R)SGVLAGHDNR(V)	513.2598	+2	18	391.6988, 598.2692, 669.3063, 782.3904
		(R)SGVLAGHDNR(V)	342.5089	+3	15	335.1568, 391.6988, 441.2330, 469.7438
$G\beta_5$	45−54	(R)VEALGQFVMK(T)	561.3048	+2	20	709.3702, 822.4542, 893.4913, 1022.5339
		(R)VEALGQFV**M**K(T)	569.3023	+2	20	540.2850, 725.3651, 838.4491, 909.4863
	87−97	(K)VIVWDSFTTNK(E)	655.3430	+2	23	679.3515, 812.3785, 998.4578, 1097.5262
	280−296	(K)ESIIFGASSVDFSLSGR(L)	886.4467	+2	30	666.3570, 781.3839, 967.4843, 1054.5164
	318−327	(R)VSILFGHENR(V)	586.3146	+2	21	493.2643, 612.2848, 759.3533, 872.4373
$G\gamma_2$	21−27	(K)MEANIDR(I)	424.7002	+2	16	517.2729, 588.3100, 717.3526
		(K)**M**EANIDR(I)	432.6976	+2	16	517.2729, 588.3100, 717.3526
	33−46	(K)AAADLMAY**C**EAHAK(E)	761.3449	+2	26	715.3192, 878.3825, 1080.4601, 1193.5442
		(K)AAADL**M**AY**C**EAHAK(E)	769.3423	+2	26	698.3052, 878.3825, 949.4196, 1096.4550
	47−62	(K)EDPLLTPVPASENPFR(E)	891.4571	+2	30	769.4223, 917.4476, 1113.5687, 1214.6164
$G\gamma_3$	3−17	(K)GETPVNSTMSIGQAR(K)	774.3778	+2	26	431.2361, 544.3202, 630.8219, 681.3457, 950.4724, 1064.5153
		(K)GETPVNST**M**SIGQAR(K)	782.3752	+2	26	431.2361, 638.8193, 689.3432, 1080.5102
	25−31	(K)IEASLCR(I)	424.7184	+2	16	448.2337, 535.2657, 606.3028, 735.3454
$G\gamma_4$	3−17	(K)EGMSNNSTTSISQAR(K)	791.8599	+2	27	431.2467, 661.3628, 863.4581, 950.4901
		(K)EG**M**SNNSTTSISQAR(K)	799.8574	+2	27	461.2467, 574.3307, 661.3628, 863.4581
	34−50	(K)VSQAASDLLAY**C**EAHVR(E)	630.6440	+3	26	717.3457, 752.8643, 788.3828, 8959281
	51−66	(R)EDPLIIPVPASENPFR(E)	897.4753	+2	30	917.4476, 1113.5687, 1226.6528
$G\gamma_5$	28−36	(K)VSQAAADLK(Q)	451.7507	+2	17	260.1969, 358.7005, 588.3352, 803.4258
	64−68	(K)V**C**SFL(-)	625.3014	+2	22	279.1703, 366.2023, 526.2330
$G\gamma_7$	19−25	(R)IEAGIER(I)	394.2191	+2	15	474.2671, 545.3042, 674.3468
	45−60	(R)NDPLLVGVPASENPFK(D)	848.9489	+2	28	734.4139, 889.4414, 1045.5313, 1144.5997
$G\gamma_{11}$	17−23	(K)MEVEQLR(K)	425.7315	+2	17	416.2616, 545.3042, 644.3726, 773.4152
		(K)**M**EVEQLR(K)	460.7289	+2	17	416.2616, 545.3042, 644.3726, 773.4152
	42−47	(K)NYIEER(S)	823.3945	+2	28	278.1135, 304.1615, 391.1976, 520.2402,
$G\gamma_{12}$	5−15	(K)TASTNSIAQAR(R)	560.2913	+2	20	445.2515, 645.3678, 759.4108, 947.4905
	23−29	(R)LEASIER(I)	409.2243	+2	15	504.2776, 575.3148, 704.3573
	49−64	(R)SDPLLMGIPTSENPFK(D)	873.4426	+2	29	772.4131, 919.4520, 1089.5575, 1220.5980
		(R)SDPLL**M**GIPTSENPFK(D)	881.4400	+2	29	780.4105, 919.4520, 1089.5575, 1236.5929
$G\gamma_{13}$	18−23	(K)YQLAFK(R)	385.2158	+2	15	365.2183, 478.3024, 606.3610
	37−44	(K)WIEDGIPK(D)	479.2556	+2	17	244.1656, 414.2711, 529.2980, 658.3406
	55−61	(K)NNPWVEK(A)	443.7245	+2	16	276.1554, 386.7030, 658.3559

[a]Bold letters C and M represent carbidomethylation and oxidation of cysteine and methionine, respectively.

fractions during discovery experiments. Polymorphisms in the $G\beta_3$ gene have been shown to dramatically alter its amino acid sequence;[66] $G\gamma_8$ is expressed only in olfactory and vomeronasal neuroepithelia,[67] and $G\gamma_{10}$ is only a minor isoform in the CNS.[41] Such factors may account for why we were unable to identify unique peptides using published sequences. These isoforms were excluded from the targeted LC−MS/MS analysis. Further, $G\gamma_1$ was not investigated, as its expression is limited to the retina.[68] Figure 2B shows a representative spectrum for the LC−MS/MS identification of a $G\beta_1$ peptide, ACADATLSQITNNIDPVGR. Gβγ precursor peptides with appropriate m/z values (<5 ppm relative to theoretical values) were fragmented to generate MS/MS spectra. Unique precursor peptides identified in data-dependent runs were verified by manual interrogation of the MS/MS spectra and product ions ranked on the basis of intensity. Discovery experiments were leveraged such that isoform specific peptides showing both a strong signal and fragmentation were chosen as precursors and transitions for monitoring via MRM. Chromatographic peaks were selected using criteria previously described. If purified samples were available, the RTs of peptides identified in complex mixtures had to match the RTs for those of the purified sample (Figure 2C). Similarly, relative intensities of transitions were required to mirror those of purified samples

dx.doi.org/10.1021/bi500091p | Biochemistry 2014, 53, 2329−2343

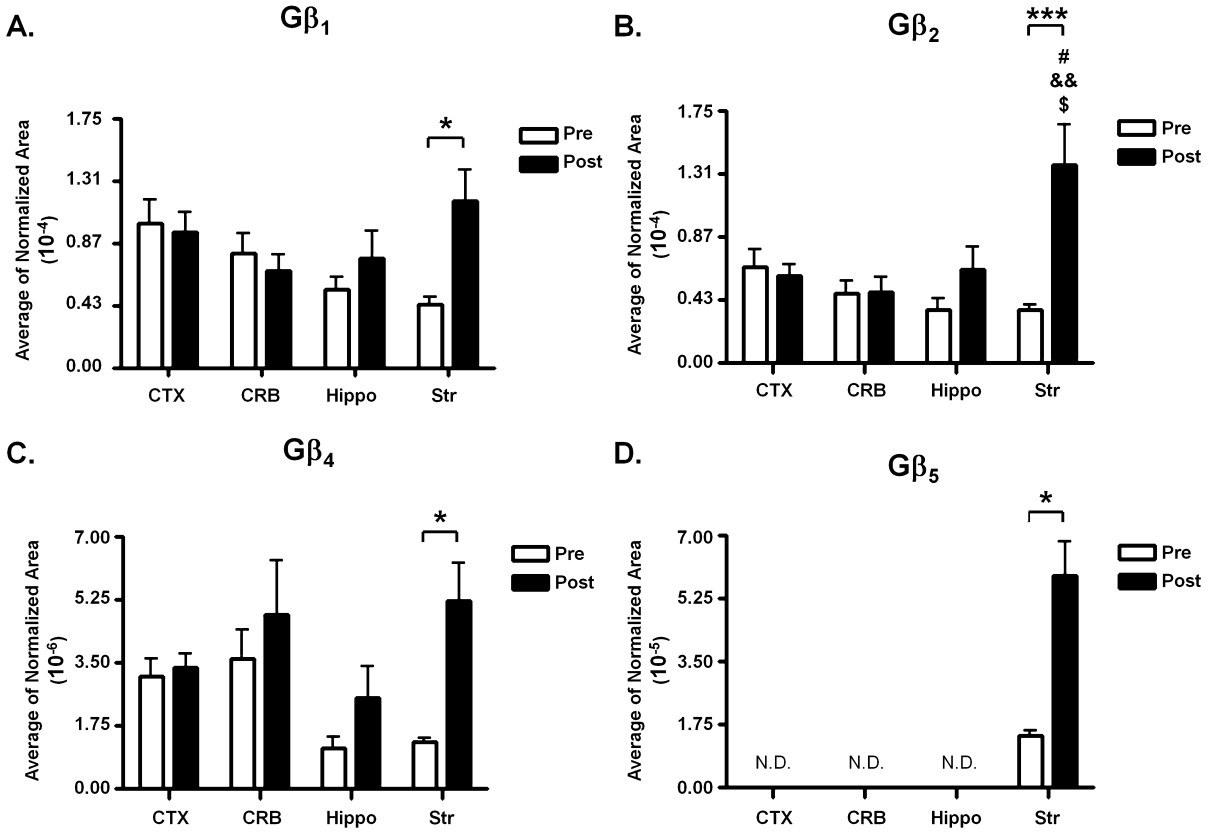

Figure 3. Gβ isoforms exhibit differential regional and subcellular localization patterns within the mouse brain. Expression of specific Gβ isoforms (A) Gβ_1, (B) Gβ_2, (C) Gβ_4, and (D) Gβ_5 in cortex, cerebellum, hippocampus, and striatum. Data for panels A–C were compared by a two-way ANOVA. The two-way ANOVA results were as follows: (A) Gβ_1, interaction effect $p = 0.0321$; (B) Gβ_2, brain region affect $p = 0.0362$, fraction effect $p = 0.0039$, and interaction effect $p = 0.0023$; (C) Gβ_4, fraction effect $p = 0.0066$. Post hoc analysis was achieved by Tukey's multiple-comparison test. *$p < 0.05$. **$p < 0.01$. ***$p < 0.001$. ****$p < 0.0001$. Data for panel D were evaluated by an unpaired t test ($p = 0.01$). Comparison to cortex represented by #, to cerebellum by &, and to hippocampus by $. Significance for each symbol as indicated for asterisks. N.D., not detected. $N = 4$ for all brain regions.

and correlate closely with that seen in discovery experiments (Figure 2C). Dot plot values were used as an aid to assess how well MRM results matched MS/MS data obtained with the Orbitrap. MRM methods were refined to pare down the number of peptides and transition ions being evaluated. Table 2 shows the list of finalized precursor peptides and product ions being monitored in MRM experiments for each G protein isoform in experimental samples.

Evaluating Regional and Subcellular G Protein Localization Patterns. We next applied our refined MRM method to subcellular fractions isolated from mouse cortex, cerebellum, hippocampus, and striatum. All four of the β isoforms (Gβ_1, Gβ_2, Gβ_4, and Gβ_5) being targeted were detected in pre- and postsynaptic fractions in all four brain regions, as well as six of the eight γ isoforms (Gγ_2, Gγ_3, Gγ_4, Gγ_7, Gγ_{12}, and Gγ_{13}). Chromatographic peaks of monitored transition ions could not be confidently identified for Gγ_5 and Gγ_{11} despite the fact that target peptides had been validated using recombinant proteins in the development phase. Gγ_{11} is thought to be a minor isoform in the brain with the highest level of expression in lung and platelets.[41] Further, both Gγ_5 and Gγ_{11} undergo post-translational processing;[41,69] this was not included in method development and could explain why peptides could not be confidently identified in CNS fractions. Neither isoform was included in analyses. No significant variance in system performance was observed across quality control (QC) runs as measured by examining BSA peptide peak areas across the experiment or peak area coefficients of variation (CVs) for replicate QC analyses (Figure 1 of the Supporting Information). Similarly, no significant drift in assay performance was observed as measured by monitoring peak areas as well peak area CVs for internal reference peptides (Figures 2 and 3 of the Supporting Information). Although stable isotope dilution (SID) is the gold standard for quantifying protein expression,[64,70] its cost-prohibitive nature prevented its use when trying to evaluate a large number of G protein isoforms. Instead, application of an LRP method[64] allowed the relative abundance of G protein isoforms to be examined. With this method, direct comparisons between isoforms cannot be made; rather, comparisons are only possible across brain regions and subcellular fractions for each individual isoform, as described below. As a result, average normalized areas for each isoform were each plotted on different axes in Figures 3 and 4.

Gβ Isoforms. Subcellular localization patterns were evaluated for each of the four Gβ isoforms being monitored by MRM. Although there was a trend toward higher levels of expression of Gβ_1 and Gβ_4 in the cortex and cerebellum, expression levels were not significantly different within or across most brain regions for three of the four isoforms (Figure 3A–C). Within the striatum, however, Gβ_1, Gβ_2, and Gβ_4 were all expressed at significantly higher levels in the postsynaptic fraction than in the presynaptic fraction (Figure 3A–C). An

dx.doi.org/10.1021/bi500091p | Biochemistry 2014, 53, 2329–2343

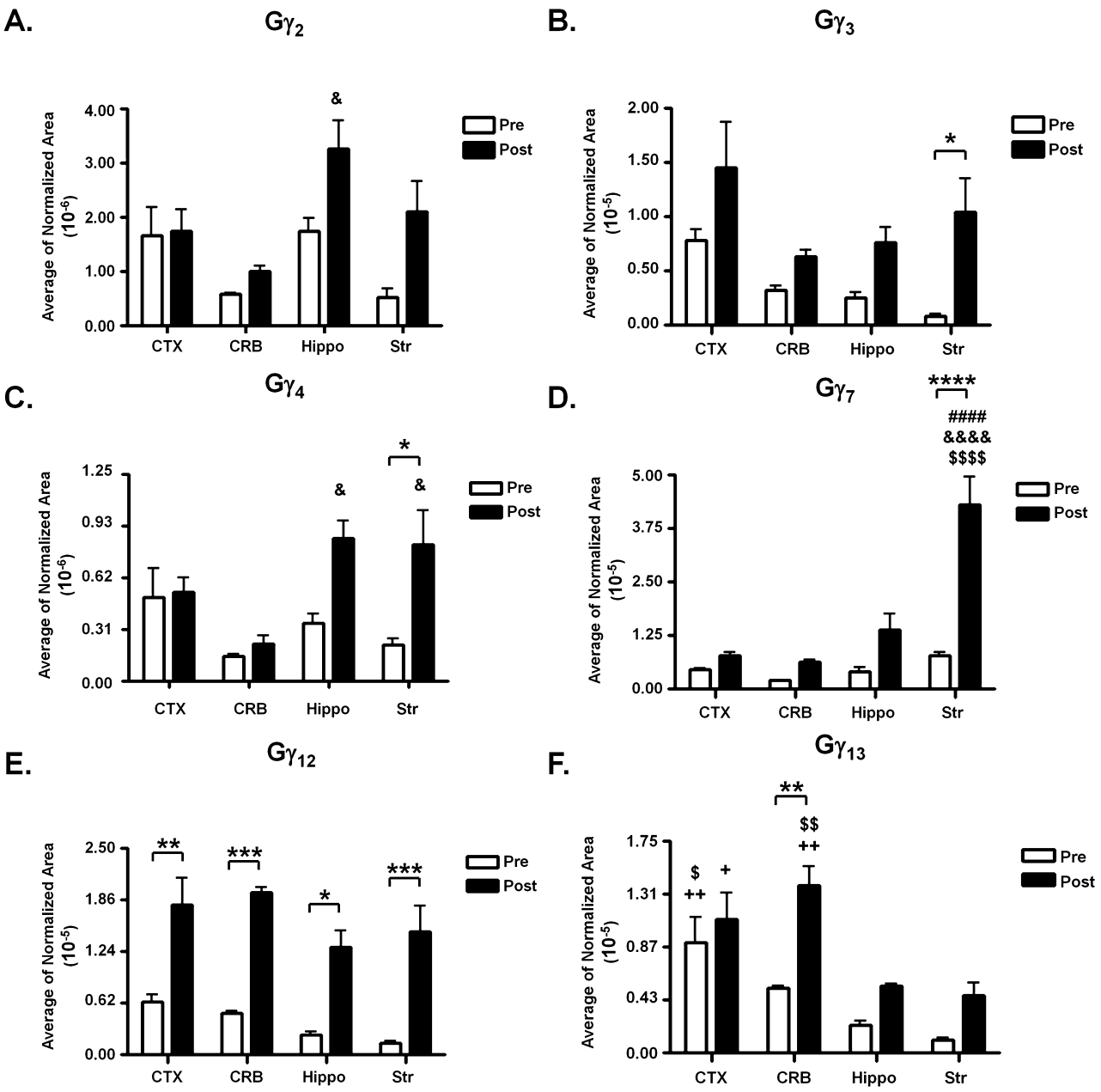

Figure 4. Gγ isoforms exhibit differential regional and subcellular localization patterns within the mouse brain. Expression of specific Gγ isoforms (A) Gγ_2, (B) Gγ_3, (C) Gγ_4, (D) Gγ_7, (E) Gγ_{12}, and (F) Gγ_{13} in cortex, cerebellum, hippocampus, and striatum. Data were compared by a two-way ANOVA. The two-way ANOVA results were as follows: (A) Gγ_2, brain region effect $p = 0.002$ and fraction effect $p = 0.0035$; (B) Gγ_3, brain region effect $p = 0.0125$ and fraction effect $p = 0.0003$; (C) Gγ_4, brain region effect $p = 0.0093$, fraction effect $p = 0.001$, and interaction effect $p = 0.04$; (D) Gγ_7, brain region effect $p < 0.0001$, fraction effect $p < 0.0001$, and interaction effect $p < 0.0001$; (E) Gγ_{12}, brain region effect $p = 0.0304$ and fraction effect $p < 0.0001$; (F) Gγ_{13}, brain region effect $p < 0.0001$ and fraction effect $p < 0.0001$. Post hoc analysis was achieved by Tukey's multiple-comparison test. *$p < 0.05$. **$p < 0.01$. ***$p < 0.001$. ****$p < 0.0001$. Comparison to cortex represented by #, to cerebellum by &, to hippocampus by $, and to striatum by +. Significance for each symbol as indicated for asterisks. $N = 4$ for all brain regions.

interaction effect was seen for Gβ_1 (ANOVA p value = 0.0321), specifically, a Gβ_1 Str post/Str pre fold difference of 2.63, with a p value of <0.05 (Table 1 of the Supporting Information), whereas there were brain region, fraction, and interaction effects for Gβ_2 [ANOVA p values of 0.0362, 0.0039, and 0.0023, respectively; Gβ_2 Str post/Str pre fold difference of 3.78, with a p value of <0.001 (Table 2 of the Supporting Information)] and a fraction effect for Gβ_4 [ANOVA p value = 0.0066; Str post/Str pre fold difference of 4.06, with a p value of <0.05 (Table 3 of the Supporting Information)]. In addition, the level of postsynaptic expression of Gβ_2 was significantly greater in the striatum than in postsynaptic fractions from the cortex, cerebellum, or hippocampus [Figure 3B; Str post/CTX post fold difference of 1.55, with a p value of <0.05; Str post/CRB post fold difference of 1.08, with a p value of <0.01; Str post/Hippo post fold difference of 2.08, with a p value of <0.05 (Table 2 of the Supporting Information)]. In comparison, Gβ_5 was detected in only the striatum on the basis of our peak criteria and S/N requirements (Figure 3D). As was seen for the other Gβ isoforms, the level of expression of Gβ_5 was significantly higher in the postsynaptic fraction than in the presynaptic fraction [Figure 3D; Str post/Str pre fold difference

dx.doi.org/10.1021/bi500091p | Biochemistry 2014, 53, 2329−2343

of 4.07, with a p value of <0.05 (Table 4 of the Supporting Information)].

Gγ Isoforms. In contrast to the Gβ isoforms, the Gγ isoforms showed greater diversity in their subcellular and regional localization patterns. $G\gamma_2$, $G\gamma_3$, $G\gamma_4$, $G\gamma_7$, $G\gamma_{12}$, and $G\gamma_{13}$ were clearly detected in each of the four brain regions being studied. In the case of $G\gamma_2$, no significant differences in regional or subcellular fractions were observed, except within the hippocampus. The level of expression of this isoform was found to be significantly greater in the postsynaptic fraction of the hippocampus than in the cerebellum (Figure 4A). There were brain region and fraction effects for $G\gamma_2$ (ANOVA p values of 0.002 and 0.0035, respectively), specifically, a $G\gamma_2$ Hippo post/CRB post fold difference of 3.61, with a p value of <0.05 (Table 5 of the Supporting Information). Additionally, there was a trend toward higher levels of expression in the postsynaptic fraction of the hippocampus and striatum compared to presynaptic fractions within these same regions (Figure 4A). Similar patterns of expression were observed for $G\gamma_3$. No significant differences were observed across the four brain regions. When comparisons were made between subcellular fractions, however, there was a trend toward higher levels of expression in postsynaptic fractions, although this was only significant within the striatum (Figure 4B). In this case, there were also brain region and fraction effects (ANOVA p values of 0.0125 and 0.0003, respectively), specifically, a $G\gamma_3$ Str post/Str pre fold difference of 2.60, with a p value of <0.05 (Table 6 of the Supporting Information). $G\gamma_4$ and $G\gamma_7$ were somewhat different in that significant differences were observed in both regional and subcellular expression. There were brain region, fraction, and interaction effects for both isoforms ($G\gamma_4$ ANOVA p values of 0.0093, 0.001, and 0.04, respectively; $G\gamma_7$ ANOVA p value of <0.0001 for all three effects). In the case of $G\gamma_4$, the level of postsynaptic expression in the hippocampus and striatum was found to be significantly greater than that in the cerebellum [Figure 4C; Hippo post/CRB post fold difference of 4.00, with a p value of <0.05; Str post/CRB post fold change of 3.83, with a p value of <0.05 (Table 7 of the Supporting Information)]. Further, while there was a trend toward a higher level of expression in the postsynaptic fraction than in the presynaptic fraction within both the hippocampus and striatum, it was only significant within the striatum [Figure 4C; Str post/Str pre fold difference of 3.71, with a p value of <0.05 (Table 7 of the Supporting Information)]. Expression of $G\gamma_7$ was not significantly different between pre- and postsynaptic fractions in the cortex, cerebellum, and hippocampus. Within the striatum, however, the level of expression was significantly higher in the postsynaptic fraction than in the presynaptic fraction [Figure 4D; Str post/Str pre fold difference of 5.55, with a p value of <0.0001 (Table 8 of the Supporting Information)]. Further, the level of postsynaptic expression of this isoform was significantly higher in the striatum than in the postsynaptic fraction in each of the other three brain regions [Figure 4D; Str post/CTX post fold difference of 5.47, with a p value of <0.0001; Str post/CRB post fold difference of 8.41, with a p value of <0.0001; Str post/Hippo post fold difference of 3.13, with a p value of <0.0001 (Table 8 of the Supporting Information)]. $G\gamma_{12}$ was unique among the isoforms in that although no regional differences were observed, the level of subcellular expression was significantly higher in postsynaptic fractions across all brain regions than in presynaptic fractions (Figure 4E). There were brain region and fraction effects for $G\gamma_{12}$ [CTX post/CTX pre fold difference of 2.81, with a p value of <0.01; CRB post/CRB pre fold difference of 3.16, with a p value of <0.001; Hippo post/Hippo pre fold change of 5.36, with a p value of <0.05; Str post/Str pre fold difference of 10.46, with a p value of <0.001 (Table 9 of the Supporting Information)]. Finally, $G\gamma_{13}$ exhibited both regional and subcellular differences in localization, and there were both brain region and fraction effects for this isoform (ANOVA p value of <0.0001 in both cases). The level of expression of this isoform in the cortex was found to be significantly higher in both the pre- and postsynaptic fractions than in the hippocampus and striatum [Figure 4F; CTX pre/Hippo pre fold difference of 4.03, with a p value of <0.05; CTX pre/Str pre fold difference of 8.76, with a p value of <0.01; CTX post/Str post fold difference of 2.86, with a p value of <0.05 (Table 10 of the Supporting Information)]. Similarly, the level of expression of $G\gamma_{13}$ was found to be significantly higher in the postsynaptic fraction of the cerebellum than in the postsynaptic fractions of the hippocampus and striatum [Figure 4F; CRB post/Hippo post fold difference of 2.38, with a p value of <0.01; CRB post/Str post fold difference of 3.06, with a p value of <0.01 (Table 10 of the Supporting Information)]. No significant differences in subcellular localization were observed in the cortex, hippocampus, or striatum, but the level of expression was significantly higher in the postsynaptic fraction within the cerebellum than in the presynaptic fraction [Figure 4F; CRB post/CRB pre fold difference of 2.22, with a p value of <0.01 (Table 10 of the Supporting Information)].

DISCUSSION

G protein βγ subunits are known to play essential roles in cellular communication via complex regulatory mechanisms. Increasingly, studies are demonstrating that receptors and effectors preferentially interact with unique complements of Gβγ isoforms,[23,24,43,71−73] suggesting that precise regulation of expression and localization is important[74] for maintaining the fidelity of signaling pathways. Transcript expression suggests these isoforms are distributed across many brain regions, but less is known about protein localization as a high level of sequence identity makes development of subunit specific antibodies difficult. The novel application of MRM techniques to this question allows accurate identification and quantification of endogenous Gβγ subunits from complex mixtures of brain tissue. With this approach, we demonstrate brain region specific differences in the protein expression patterns of individual G protein β and γ isoforms in pre- and postsynaptic fractions. We employed an LRP method to evaluate the relative expression of each isoform, as SID methods that include labeled internal protein standards for each peptide being monitored are cost-prohibitive given the number of peptides to be analyzed. Zhang et al.[64] recently showed that an LRP method is a reasonable alternative to SID as it is well suited for comparing relative protein levels and is capable of detecting the same significant differences in biological samples. Application of this technique to this study is a first required step toward a more complete understanding of specificity in Gβγ signaling. The observed differences suggest neuronal cells would be able to channel information differentially through signaling complexes and second-messenger pathways in different brain regions.

Differential Expression and Distribution of Gβγ Isoforms between Brain Regions. Several studies have demonstrated that Gβ and Gγ isoforms show differential patterns of expression throughout the CNS. Although the data obtained in those studies are in general agreement with those

presented here, ours is the first to provide a comprehensive map of their protein distribution to distinct subcellular fractions; previously, only $G\beta_1$ has been reported in both the presynaptic active zone[55] and PSD.[56] $G\beta_1$ is expressed ubiquitously throughout the brain,[35,39] correlating well with our findings that this isoform could be detected at comparable levels within pre- and postsynaptic fractions across most of the brain regions examined (Figure 3A). A similar range of levels of expression was observed for $G\beta_2$ and $G\beta_4$ (Figure 3B,C). *In vitro* data show that $G\beta_1$, $G\beta_2$, and $G\beta_4$ can all pair with numerous $G\gamma$ isoforms, as well as couple to a variety of receptors and effectors.[75] While this implies involvement in a wide range of signaling pathways and supports the broad distribution we observed, their function *in vivo* is poorly understood. What is known is that $G\beta_1$ plays an important role in neural development; its removal is perinatally lethal, and pups exhibit reduced cortical thickness, reduced brain volume, and impaired neural progenitor cell proliferation.[76] Comparatively, $G\beta_2$ may play a role in neuronal excitability as mice in which $G\gamma3$ is lost exhibit a severe seizure phenotype and a reduction in the level of $G\beta_2$ within the cortex, cerebellum, and striatum.[25,77] Further, knockdown studies demonstrate $G\beta_1$, $G\beta_2$, and $G\beta_4$ each signal downstream of specific GPCRs found throughout the CNS.[78,79] The extensive expression patterns we observed for each isoform may thus be expected, as a broad distribution would be required to support such diverse signaling pathways.

In contrast to the other $G\beta$ isoforms, expression of $G\beta_5$ was seen exclusively within the striatum, as levels within the cortex, cerebellum, and hippocampus were below the limit of detection (Figure 3D). This result differs from previously published reports that suggested a wide distribution similar to that of the other $G\beta$ isoforms.[35,39,40] While we cannot rule out that such disparity reflects physiological differences in the expression of the protein product or differential post-translational processing between brain regions, such a limited distribution may also correspond to the interaction of $G\beta_5$ with regulators of G protein signaling (RGS) proteins. $G\beta_5$ forms a stable obligate dimer with members of the RGS R7 subfamily to modulate G_i-mediated signal transduction pathways.[80−84] One member, RGS9-2, is enriched in the striatum, and the RGS9-2−$G\beta_5$ complex is localized to the membrane through its interaction the R7 family binding protein (R7BP).[82,85−87] Conversely, RGS7−Gβ5 complexes are found intracellularly throughout the CNS.[82,87] This may explain why, in this study, $G\beta_5$ could be detected only in the striatum. Our fractionation protocol aimed to enrich the presynaptic active zone membrane fraction as well as the PSD membrane fraction, while cytosolic fractions were not analyzed. The $G\beta_5$−RGS9-2 association with the plasma membrane in the striatum is consistent with our detection of $G\beta_5$ in this region. Further, as R7BP and RGS9-2 colocalize predominantly to postsynaptic membranes,[86,88] enrichment of $G\beta_5$ in postsynaptic fractions within this region would be expected (Figure 3D). If, in other brain regions, $G\beta_5$ is primarily complexed with RGS7 and found intracellularly, it would not have been detected in this study as these fractions were not analyzed. Further efforts will be needed to determine whether $G\beta_5$ can be detected in cytosolic fractions to address this hypothesis.

In comparison, the $G\gamma$ subunits show more varied expression patterns; however, with the exception of $G\gamma_5$ and $G\gamma_{11}$, each isoform could be clearly identified within each of the four brain regions examined (Figure 4). Although immunohistochemical studies have localized particular isoforms to the CNS in general, a detailed examination of their expression to brain regions and cell types has been limited to transcript levels.[35,89] For some $G\gamma$ isoforms, transcript expression reported previously correlates well with the localization patterns observed in this study, whereas in others it differs notably. For example, using *in situ* hybridization, Betty et al.[35] showed strong expression of $G\gamma_7$ within the striatum, followed closely by the hippocampus, cortex, and cerebellum, similar to what is seen in this study (Figure 4D). Conversely, the authors reported $G\gamma_4$ to be strongly expressed in the hippocampus and cerebellum but more weakly in the striatum, whereas our analyses show the opposite: strong expression in the striatum but significantly lower levels in the cerebellum (Figure 4C). It is difficult to say whether these differences reflect physiological effects relating to the expression of the protein product or possible protein modifications that were not identified in this study. One factor that may contribute to the disparities, however, is that this study examined expression patterns at subcellular levels. In comparison, previous *in situ* studies were able to evaluate $G\gamma$ expression at only the cellular level, which would have included both the soma and the nerve terminals. Thus, direct comparison between such studies is not possible.

Little is known about the subcellular distribution of $G\gamma$ isoforms within the CNS. Moricano et al.[55] localized $G\gamma_3$ to the presynaptic active zone, but subcellular localization patterns for the remaining $G\gamma$ isoforms have not been previously evaluated. The wide discrepancy in expression patterns within subcellular fractions and across the four brain regions could reflect unique contributions by each isoform to unique signaling pathways. This is supported by the distinct phenotypes observed when $G\gamma$ isoforms are genetically knocked out. In the case of $G\gamma_3$, genetic deletion results in mice with an increased susceptibility to seizures, as well as resistance to diet-induced obesity, implying a role in neuronal excitability and regulation of appetite or metabolism.[24,77] Loss of $G\gamma_3$ suppresses the expression of $G\beta_1$ and $G\beta_2$ within the cortex, cerebellum, and striatum, implicating a $G\beta_{1/2}\gamma_3$ dimer within these regions and in agreement with our expression results (Figure 4B). It is noteworthy that significant enrichment of $G\gamma_3$ was observed in the postsynaptic fraction of the striatum. Although further efforts are needed to understand the physiological consequences of this finding, one possibility may be related to the activity of μ-opioid receptors within this region. The loss of $G\gamma_3$ results in defective signaling through the μ-opioid receptor.[77] Within the striatum, these receptors have been implicated in the hedonic response to food[90,91] and act via a postsynaptic mechanism.[92] As a result, the enrichment seen in the postsynaptic fraction of the striatum could represent an important signaling cascade activated by μ-opioid receptors and involving the $G\gamma_3$ subunit; further efforts will be needed to explore this possibility. In comparison, animals in which $G\gamma_7$ has been knocked out exhibit an enhanced startle response, which may result from defective D_1 dopamine and A_{2A} adenosine receptor activation within the striatum.[25,93,94] This correlates well with our finding, and previously published reports,[35,95] that $G\gamma_7$ is most strongly expressed in the striatum (Figure 4D). While further efforts will be needed to confirm the exact mechanism, given that both D_1 and A_{2A} receptors are localized primarily to dendritic spines,[96,97] the fact that we observed significant enrichment of $G\gamma_7$ within the postsynaptic fraction (Figure 4D) suggests a predominately postsynaptic role for $G\gamma_7$ within this region.

Although no genetically modified animals are available for $G\gamma_2$ and $G\gamma_4$, knockdown of these isoforms offers insight into the expression patterns we observed. Early work by Kalkbrenner et al.[98] demonstrated that silencing of endogenous $G\gamma_2$ and $G\gamma_4$ in cultured cells reduced the extent of galanin-induced calcium inhibition. More recently, a role in nociception was suggested for $G\gamma_2$, as injection of antisense oligonucleotides into the CNS of mice attenuated the analgesic effects of opioid, cannabinoid, and adrenergic agonists.[99,100] Such a range of effector interactions would be expected to contribute to the observed localization patterns. Galanin, cannabinoid, and adrenergic receptors all exhibit a broad distribution in the CNS,[101] while opioid receptor subtypes are highly expressed within the striatum and cortex.[102−104] As a result, if $G\gamma_2$ and $G\gamma_4$ acted via these receptors *in vivo*, the wide distribution we observed (Figure 4A,C) could exist because their expression parallels that of their target GPCRs.

Finding $G\gamma_{13}$ within each of the brain regions we examined was exciting as this G protein has largely been reported in sensory tissues, where it is required for olfactory and gustatory transduction.[105] While transcript expression within the brain closely mirrors our results[106,107] (Figure 4F), little is known about the function of this isoform in the CNS. $G\gamma_{13}$ has been shown to interact with the third PDZ domain of PSD-95 via a PDZ binding C-terminal sequence, and the two proteins can be efficiently pulled down together from brain lysates.[108] It is possible that this association aids in targeting the G protein to particular subcellular locations and/or facilitates interactions with appropriate effectors such as GIRK channels and $PLC\beta_2$,[106] accounting for the stronger expression of $G\gamma_{13}$ in postsynaptic fractions (Figure 4F).

Additional Factors That May Contribute to Differential Expression Patterns. In addition to signaling requirements, other factors are likely to influence the observed localization patterns. A striking feature from our data was that while most G protein isoforms were found in all four brain regions, prominent differences were observed between regions. Such disparity may reflect G protein expression within individual cell types as well as patterns of innervation to specific brain regions. For example, the striatum is composed largely of γ-aminobutyric acid (GABA)-containing medium spiny neurons yet receives excitatory inputs from the cortex and dopaminergic innervations from the midbrain.[109,110] Glutamatergic pyramidal neurons predominate in the hippocampus, but this region also receives monoamine and cholinergic inputs from the median raphe,[111,112] locus coeruleus,[113] and basal forebrain.[114] In contrast, the cerebellum could be considered more homogeneous as Purkinje cells represent the sole output of the cerebellar cortex, but even these integrate excitatory afferent pathways as well as strong inhibitory GABAergic inputs.[115] Such diversity in cell type and innervation patterns may provide clues about why differences in G protein expression patterns were observed between brain regions as well as subcellular fractions. This is supported by early work by Betty et al.[35] and Liang et al.,[39] as well as the more recent effort or Schwindinger et al.[25] Thus, G protein expression within particular cell types, as well as the innervation within a brain region, would influence the results seen in our study. Synaptosomal preparations and subcellular fractionation techniques such as those described do not allow $G\beta\gamma$ expression patterns to be evaluated endogenously within specific cell types. However, with recent advances in optogenetics, transgenic mice that express fluorescent proteins under the control of cell-type specific promoters are becoming available. By taking advantage of these mice in future studies, we will be able to evaluate localization patterns within specific neuron populations and subcellular fractions to determine if these factors contribute to the expression of specific isoforms.

SUMMARY

In summary, we report that G protein β and γ isoforms exhibit distinct patterns of localization across brain regions as well as subcellular fractions. This is particularly interesting as it implies specific functions for individual isoforms in modulating cellular responses and signaling cascades. Further efforts will be necessary to determine the relevance of these patterns of distribution and to evaluate which $G\beta\gamma$ dimers exist endogenously and the contribution each makes to cellular communication.

ASSOCIATED CONTENT

Supporting Information

Tables detailing BSA and internal reference peptide quality control peak areas and coefficients of variation and figures showing how fold differences were calculated. This material is available free of charge via the Internet at http://pubs.acs.org.

AUTHOR INFORMATION

Corresponding Author

*Department of Pharmacology, Vanderbilt University Medical Center, 442 Robinson Research Building, 23rd Ave. South @ Pierce, Nashville, TN 37232-6600. E-mail: heidi.hamm@vanderbilt.edu. Telephone: (615) 343-3533. Fax: (615) 343-1084.

Funding

This work was supported by the National Eye Institute (RO1 EY010291 to H.E.H.), a Vanderbilt CTSA grant from the National Center for Research Resources (UL1 RR024975-01 to K.M.B.), and funding from the Howard Hughes Medical Institute Med into Grad Initiative (K.M.B.) and the Philanthropic Educational Organization (K.M.B.).

Notes

The authors declare no competing financial interest.

ACKNOWLEDGMENTS

We thank Dr. Ana Carneiro (Vanderbilt University School of Medicine, Nashville, TN) for her technical assistance in preparing synaptosomes and subcellular fractions and Dr. Hayes McDonald (Vanderbilt Mass Spectrometry Research Center Proteomics Laboratory, Nashville, TN) for his advice and suggestions. We also thank members of the Hamm lab for their helpful comments and suggestions throughout this project.

ABBREVIATIONS

AUC, area under the curve; CAPS, 3-(cyclohexylamino)-1-propanonesulfonic acid; CID, collision-induced dissociation; CNS, central nervous system; CRB, cerebellum; CTX, cortex; CV, coefficient of variation; GABA, γ-aminobutyric acid; GAPDH, glyceraldehyde-3-phosphate dehydrogenase; GGL, G protein γ-like; GPCR, G protein-coupled receptor; HEPES, 4-(2-hydroxyethyl)-1-piperazineethanesulfonate; Hippo, hippocampus; LC−MS/MS, liquid chromatography and tandem mass spectrometry; LRP, labeled reference peptide; MRM, multiple-reaction monitoring; NMDAR1, *N*-methyl-D-aspartate

receptor 1; PMSF, phenylmethanesulfonyl fluoride; PLC, phospholipase C; PRE, presynaptic; PSD-95, post-synaptic density 95; PSD, postsynaptic density; R7BP, R7 family binding protein; RGS, regulators of G protein signaling; RT, retention time; SD, standard deviation; SID, stable isotope dilution; S/N, signal to noise; Str, striatum; TBS, Tris-buffered saline; TX-100, triton X-100; QC, quality control.

REFERENCES

(1) Oldham, W. M., and Hamm, H. E. (2008) Heterotrimeric G protein activation by G protein-coupled receptors. *Nat. Rev. Mol. Cell Biol. 9* (1), 60−71.

(2) Hamm, H. E. (1998) The many faces of G protein signaling. *J. Biol. Chem. 273* (2), 669−672.

(3) Tang, W. J., and Gilman, A. G. (1991) Type-specific regulation of adenylyl cylcase by G proten $\beta\gamma$ subunits. *Science 254*, 1500−1503.

(4) Clapham, D. E., and Neer, E. J. (1993) New roles for G-protein $\beta\gamma$-dimers in transmembrane signaling. *Nature 365*, 403−406.

(5) Myung, C. S., Yasuda, H., Liu, W. W., Harden, T. K., and Garrison, J. C. (1999) Role of isoprenoid lipids on the heterotrimeric G protein γ subunit in determining effector activation. *J. Biol. Chem. 274*, 16595−16603.

(6) Vanderbeld, B., and Kelly, G. M. (2000) New thoughts on the role of the $\beta\gamma$ subunit in G-protein signal transduction. *Biochem. Cell Biol. 78*, 537−550.

(7) Cabrera-Vera, T. M., Vanhauwe, J., Thomas, T. O., Medkova, M., Preininger, A., Mazzoni, M. R., and Hamm, H. E. (2003) Insights into G Protein Structure, Function, and Regulation. *Endocr. Rev. 24* (6), 765−781.

(8) Goldsmith, Z. G., and Dhanasekaran, D. N. (2007) G protein regulation of MAPK networks. *Oncogene 26* (22), 3122−3142.

(9) Herlitze, S., Garcia, D. E., Mackie, K., Hille, B., Scheuer, T., and Catterall, W. A. (1996) Modulation of Ca^{2+} channels by G-protein $\beta\gamma$ subunits. *Nature 380*, 258−262.

(10) Huang, C.-L., Slesinger, P. A., Casey, P. J., Jan, Y. N., and Jan, L. Y. (1995) Evidence that direct binding of G$\beta\gamma$ to the GIRK1 G protein-gated inwardly rectifying K^+ channel is important for channel activation. *Neuron 15* (5), 1133−1143.

(11) Blackmer, T., Larsen, E. C., Takahashi, M., Martin, T. F., Alford, S., and Hamm, H. E. (2001) G protein $\beta\gamma$ subunit-mediated presynaptic inhibition regulation of exocytotic fusion downstream of Ca^{2+} entry. *Science 292*, 293−297.

(12) Blackmer, T., Larsen, E. C., Bartleson, C., Kowalchyk, J. A., Yoon, E. J., Preininger, A. M., Alford, S., Hamm, H. E., and Martin, T. F. (2005) G protein $\beta\gamma$ directly regulates SNARE protein fusion machinery for secretory granule exocytosis. *Nat. Neurosci. 8* (4), 421−425.

(13) Currie, K. P. (2010) Inhibition of Ca^{2+} channels and adrenal catecholamine release by G protein coupled receptors. *Cell. Mol. Neurobiol. 30*, 1201−1208.

(14) Gerachshenko, T., Blackmer, T., Yoon, E. J., Bartleson, C., Hamm, H. E., and Alford, S. (2005) G$\beta\gamma$ acts at the C terminus of SNAP-25 to mediate presynaptic inhibition. *Nat. Neurosci. 8* (5), 597−605.

(15) Yoon, E. J., Gerachshenko, T., Spiegelberg, B. D., Alford, S., and Hamm, H. E. (2007) G$\beta\gamma$ interferes with Ca^{2+}-dependent binding of synaptotagmin to the soluble N-ethylmaleimide-sensitive factor attachment protein receptor (SNARE) complex. *Mol. Pharmacol. 72*, 1210−1219.

(16) Sadja, R., and Reuveny, E. (2009) Activation gating kinetics of GIRK channels are mediated by cytoplasmic residues adjacent to transmembrane domains. *Channels 3* (3), 205−214.

(17) Wells, C. A., Zurawski, Z., Betke, K. M., Yim, Y. Y., Hyde, K., Rodriguez, S., Alford, S., and Hamm, H. E. (2012) G$\beta\gamma$ inhibits exocytosis via interaction with critical residues on soluble N-ethylmaleimide-sensitive factor attachment protein-25. *Mol. Pharmacol. 82* (6), 1136−1149.

(18) Downes, G. B., and Gautam, N. (1999) The G protein subunit gene families. *Genomics 62* (3), 544−552.

(19) Hildebrandt, J. D. (1997) Role of subunit diversity in signaling by heterotrimeric G proteins. *Biochem. Pharmacol. 54* (3), 325−339.

(20) McIntire, W. E., MacCleery, G., and Garrison, J. C. (2001) The G protein β subunit is a determinant in the coupling of Gs to the β1-adrenergic and A2a adenosine receptors. *J. Biol. Chem. 276* (19), 15801−15809.

(21) Kerchner, K. R., Clay, R. L., McCleery, G., Watson, N., McIntire, W. E., Myung, C. S., and Garrison, J. C. (2004) Differential sensitivity of phosphatidylinositol 3-kinase p110γ to isoforms of G protein $\beta\gamma$ dimers. *J. Biol. Chem. 279* (43), 44554−44562.

(22) Kleuss, C., Hescheler, J., Ewel, C., Rosenthal, W., Schultz, G., and Wittig, B. (1991) Assignment of G-protein subtypes to specific receptors inducing inhibition of calcium currents. *Nature 353*, 43−48.

(23) Kleuss, C., Scherübl, H., Hescheler, J., Schultz, G., and Wittig, B. (1992) Different β subunits determine G-protein interaction with transmembrane receptors. *Nature 358*, 424−426.

(24) Wang, Q., Mullah, B. K., and Robishaw, J. D. (1999) Ribozyme approach identifies a functional association between the G protein $\beta_1\gamma_7$ subunits in the β-adrenergic receptor signaling pathway. *J. Biol. Chem. 274* (24), 17365−17371.

(25) Schwindinger, W. F., Giger, K. E., Betz, K. S., Stauffer, A. M., Sunderlin, E. M., Sim Selley, L. J., Selley, D. E., Bronson, S. K., and Robishaw, J. D. (2004) Mice with Deficiency of G Protein γ3 Are Lean and Have Seizures. *Mol. Cell. Biol. 24* (17), 7758−7768.

(26) Schwindinger, W. F., Mirshahi, U. L., Baylor, K. A., Sheridan, K. M., Stauffer, A. M., Usefof, S., Stecker, M. M., Mirshahi, T., and Robishaw, J. D. (2012) Synergistic roles for G-protein γ_3 and γ_7 in seizure susceptibility as revealed in double knock out mice. *J. Biol. Chem. 287* (10), 7121−7133.

(27) Zhang, J.-H., Pandey, M., Seigneur, E. M., Panicker, L. M., Koo, L., Schwartz, O. M., Chen, W., Chen, C.-K., and Simonds, W. F. (2011) Knockout of G protein β_5 impairs brain development and causes multiple neurologic abnormalities in mice. *J. Neurochem. 119* (3), 544−554.

(28) Downes, G. B., Copeland, N. G., Jenkins, N. A., and Gautam, N. (1998) Structure and mapping of the G protein γ_3 subunit gene and a divergently transcribed novel gene, *Gng3lg*. *Genomics 53*, 220−230.

(29) Fisher, K. J., and Aronson, N. N., Jr. (1992) Characterization of the cDNA and genomic sequence of a G protein γ subunit (γ5). *Mol. Cell. Biol. 12* (4), 1585−1591.

(30) Gautam, N., Northup, J., Tamir, H., and Simon, M. I. (1990) G protein diversity is increased by associations with a variety of γ subunits. *Proc. Natl. Acad. Sci. U.S.A. 87*, 7973−7977.

(31) Kalyanaraman, S., Kalyanaraman, V., and Gautam, N. (1995) A brain-specific G protein γ subunit. *Biochem. Biophys. Res. Commun. 216* (1), 126−132.

(32) Morishita, R., Fukada, Y., Kokame, K., Yoshizawa, T., Masuda, K., Niwa, M., Kato, K., and Asano, T. (1992) Identification and isolation of common and tissue specific geranylgeranylated γ subunits of guanine-nucleotide-binding regulatory proteins in various tissues. *Eur. J. Biochem. 210*, 1061−1069.

(33) Watson, A. J., Katz, A., and Simon, M. I. (1994) A fifth member of the mammalian G protein β-subunit family. Expression in brain and activation of the β_2 isotype of phospholipase C. *J. Biol. Chem. 269* (35), 22150−22156.

(34) Weizsäcker, E. V., Strathmann, M. P., and Simon, M. I. (1992) Diversity among the β subunits of heterotrimeric GTP-binding proteins: Characterization of a novel β subunit cDNA. *Biochem. Biophys. Res. Commun. 183* (1), 350−356.

(35) Betty, M., Harnish, S. W., Rhodes, K. J., and Cockett, M. I. (1998) Distribution of heterotrimeric G-protein β and γ subunits in the rat brain. *Neuroscience 85* (2), 475−486.

(36) Cali, J. J., Baleueva, E. A., Rybalkin, I., and Robishaw, J. D. (1992) Selective tissue distribution of G protein γ subunits, including a new form of the γ subunits identified by cDNA cloning. *J. Biol. Chem. 267* (33), 24023−24027.

(37) Jones, P. G., Lombardi, S. J., and Cockett, M. I. (1998) Cloning and tissue distribution of the human G protein β_5 cDNA. *Biochim. Biophys. Acta 1402*, 288−291.
(38) Largent, B. L., Jones, D. T., Reed, R. R., Pearson, C. A., and Snyder, S. H. (1988) G protein mRNA mapped in rat brain by in situ hybridization. *Proc. Natl. Acad. Sci. U.S.A. 85*, 2864−2868.
(39) Liang, J.-J., Cockett, M., and Khawaja, X. Z. (1998) Immunohistochemical localization of G protein β_1, β_2, β_3, β_4, β_5, and γ_3 subunits in the adult rat brain. *J. Neurochem. 71*, 345−355.
(40) Zhang, J.-H., Lai, Z., and Simonds, W. (2000) Differential expression of the G protein β_5 gene: Analysis of mouse brain, peripheral tissues, and cultured cell lines. *J. Neurochem. 75*, 393−403.
(41) Morishita, R., Ueda, H., Kato, K., and Asano, T. (1998) Identification of two forms of the γ subunit of G protein, γ_{10} and γ_{11}, in bovine lung and their tissue distribution in the rat. *FEBS Lett. 428*, 85−88.
(42) Robishaw, J. D., Kalman, V. K., Moomaw, C. R., and Slaughter, C. A. (1989) Existence of two γ subunits of the G proteins in brain. *J. Biol. Chem. 264* (27), 15758−15761.
(43) Bigler Wang, D., Shermann, N. E., Shannon, J. D., Leonhardt, S. A., Mayeenuddin, L. H., Yeager, M., and McIntire, W. E. (2011) Binding of $\beta_4\gamma_5$ by adenosine A_1 and A_{2A} receptors determined by stable isotope labeling with amino acids in cell culture and mass spectrometry. *Biochemistry 50*, 207−220.
(44) Bai, F., and Witzmann, F. A. (2007) Synaptosome Proteomics. *Subcell. Biochem. 43*, 77−98.
(45) Boyd-Kimball, D., Castegna, A., Sultana, R., Poon, H. F., Petroze, R., Lynn, B. C., Klein, J. B., and Butterfield, D. A. (2005) Proteomic identification of proteins oxidized by Aβ(1−42) in synaptosomes: Implications for Alzheimer's disease. *Brain Res. 1044*, 206−215.
(46) Burré, J., and Volknandt, W. (2007) The synaptic vesicle proteome. *J. Neurochem. 101*, 1448−1462.
(47) Fountoulaki, M. (2004) Application of proteomics technologies in the investigation of the brain. *Mass Spectrom. Rev. 23*, 231−258.
(48) Li, K. W., Hornshaw, M. P., Van der Schors, R. C., Watson, R., Tate, S., Casetta, B., Jimenez, C. R., Gouwenberg, Y., Gundelfinger, E. D., Smalla, K.-H., and Smit, A. B. (2004) Proteomics analysis of rat brain postsynaptic density. *J. Biol. Chem. 279* (2), 987−1002.
(49) Liberatori, S., Canas, B., Tani, C., Bini, L., Buonocore, G., Godovac-Zimmermann, J., Mishra, O. P., Delivoria-Papadopoulos, M., Bracci, R., and Pallini, V. (2004) Proteomic approach to the identification of voltage-dependent anion channel protein isoforms in guinea pig brain synaptosomes. *Proteomics 4*, 1335−1340.
(50) Mallei, A., Giambelli, R., Gass, P., Racagni, G., Mathé, A. A., Vollmayr, B., and Popoli, M. (2011) Synaptoproteomics of learned helpless rats involve energy metabolism and cellular remodeling pathways in depressive-like behavior and antidepressant response. *Neuropharmacology 60*, 1243−1253.
(51) Stasyk, T., and Huber, L. A. (2004) Zooming in: Fractionation strategies in proteomics. *Proteomics 4*, 3704−3716.
(52) Witzmann, F. A., Arnold, R. J., Bai, F., Hrncirova, P., Kimpei, M. W., Mechref, Y. S., McBride, W. J., Novotny, M. V., Pedrick, N. M., Ringham, H. N., and Simon, J. R. (2005) A proteomic survey of rat cerebral cortical synaptosomes. *Proteomics 5*, 2177−2201.
(53) Gylys, K. H., Fein, J. A., Yang, F., Wiley, D. J., Miller, C. A., and Cole, G. M. (2004) Synaptic changes in Alzheimer's disease: Increased amyloid-β and gliosis in surviving terminal is accompanied by decreased PSD-95 fluorescence. *Neurobiology 165* (5), 1809−1817.
(54) Morciano, M., Burré, J., Corvey, C., Karas, M., Zimmermann, H., and Volknandt, W. (2005) Immunoisolation of two synaptic vesicle pools from synaptosomes: A proteomic analysis. *J. Neurochem. 95*, 1732−1745.
(55) Morciano, M., Beckhaus, T., Karas, M., Zimmermann, H., and Volknandt, W. (2009) The proteome of the presynaptic active zone: From docked synaptic vesicles to adhesion molecules and maxi-channels. *J. Neurochem. 108*, 662−667.
(56) Satoh, K., Takeuchi, M., Oda, Y., Deguchi-Tawarada, M., Sakamato, Y., Matsubara, K., Nagasu, Y., and Takai, Y. (2002) Identification of activity-regulated proteins in the postsynaptic density fraction. *Genes Cells 7*, 187−197.
(57) Volknandt, W., and Karas, M. (2012) Proteomic analysis of the presynaptic active zone. *Exp. Brain Res. 217*, 449−461.
(58) Boja, E. S., and Rodriguez, H. (2012) Mass spectrometry-based targeted quantitative proteomics: Achieving sensitive and reproducible detection of proteins. *Proteomics 12* (8), 1093−1100.
(59) Shi, T., Su, D., Liu, T., Tang, K., Camp, D. G., II, Qian, W. J., and Smith, R. D. (2012) Advancing the sensitivity of selected reaction monitoring-based targeted quantitative proeomics. *Proteomics 12* (8), 1074−1092.
(60) Mazzoni, M. R., Malinski, J. A., and Hamm, H. E. (1991) Structural analysis of rod GTP binding protein, Gt. Limited proteolytic digestion pattern of Gt with four proteases defines monoclonal antibody epitope. *J. Biol. Chem. 266* (21), 14072−14081.
(61) Phillips, G. R., Huang, J. K., Wang, Y., Tanaka, H., Shapiro, L., Zhang, Q., Shan, W., Arndt, K., Frank, M., Gordon, R. E., Gawinowicz, A., Zhao, Y., and Colman, D. R. (2001) The presynaptic particle web: Ultrastructure, composition, dissolution, and reconstitution. *Neuron 32*, 63−77.
(62) Eng, J. K., McCormack, A. L., Yates, I., and John, R. (1994) An approach to correlate tandem mass spectral data of peptides with amino acid sequenes in a protein database. *J. Am. Soc. Mass Spectrom. 5*, 976−989.
(63) MacLean, B., Tomazela, D. M., Shulman, N., Chambers, M., Finney, G. L., Frewan, B., Kern, R., Tabb, D. L., Liebler, D. C., and MacCoss, M. J. (2010) Skyline: An open source document editor for creating and analyzing targeted proteomics experiments. *Bioinformatics 26* (7), 966−968.
(64) Zhang, H., Liu, Q., Zimmerman, L. J., Ham, A. J., Slebos, R. J. C., Rahman, J., Kikuchi, T., Massion, P. P., Carbone, D. P., Billheimer, D., and Liebler, D. C. (2011) Methods for peptide and protein quantitation by liquid chromatography-multiple reaction monitoring mass spectrometry. *Mol. Cell. Proteomics 10* (6), M110.006593.
(65) Tobin, V., Schwab, Y., Lelos, N., Onaka, T., Pittman, Q. J., and Ludwig, M. (2012) Expression of exocytosis proteins in rat supraoptic nucleus neurones. *J. Neuroendocrinol. 24* (4), 629−641.
(66) Daimon, M., Sato, H., Kain, W., Tada, K., Takase, K., Karasawa, S., Wada, K., Kameda, W., Susa, S., Oizumi, T., Kayama, T., Muramatsu, M., and Kato, T. (2013) Association of the G-protein β_3 subunit gene polymorphism with the incidence of cardiovascular disease independent of hypertension: The Funagata study. *J. Hum. Hypertens. 27*, 612−616.
(67) Ryba, N. J. P., and Tirindelli, R. (1995) A novel GTP-binding protein g-subunit, Gγ_8, is expressed during neurogenesis in the olfactory and vomeronasal neuroepithelia. *J. Biol. Chem. 270* (12), 6757−6767.
(68) Hurley, J. B., Fong, H. K. W., Teplow, D. B., Dreyer, W. J., and Simon, M. I. (1984) Isolation and characterization of a cDNA clone for the γ subunit of bovine retinal transducin. *Proc. Natl. Acad. Sci. U.S.A. 81*, 6948−6952.
(69) Kilpatrick, E. L., and Hildebrandt, J. D. (2007) Sequence dependence and differential expression of Gγ_5 subunit isoforms of the heterotrimeric G proteins variably processed after prenylation in mammalian cells. *J. Biol. Chem. 282* (19), 14038−14047.
(70) Kirkpatrick, D. S., Gerber, S. A., and Gygi, S. P. (2005) The absolute quantification strategy: A general procedure for the quantification of proteins and post translational modificiations. *Methods 35*, 265−273.
(71) Stehno-Bittel, L., Krapivinsky, G., Krapivinsky, L., Perez-Terzic, C., and Clapham, D. E. (1995) The G protein $\beta\gamma$ subunit transduces the muscarinic receptor signal for Ca^{2+} release in *Xenopus* oocytes. *J. Biol. Chem. 270* (50), 30068−30074.
(72) Lindorfer, M. A., Myung, C. S., Savino, Y., Yasuda, H., Khazan, R., and Garrison, J. C. (1998) Differential activity of the G protein $\beta5\gamma2$ subunit at receptors and effectors. *J. Biol. Chem. 273* (51), 34429−34436.
(73) Lim, W. K., Myung, C. S., Garrison, J. C., and Neubig, R. R. (2001) Receptor-G protein gamma specificity: $\gamma11$ shows unique

potency for A_1 adenosine and $5HT_{1A}$ receptors. *Biochemistry 40* (35), 10532−10541.
(74) Hamid, E., Church, E., Wells, C. A., Zurawski, Z., Hamm, H. E., and Alford, S. (2014) Modulation of neurotransmision by GPCRs is dependant upon the microarchitecture of the primed vesicle complex. *J. Neurosci. 34* (1), 260−274.
(75) Albert, P. R., and Robillard, L. (2002) G protein specificity: Traffic direction required. *Cell. Signalling 14*, 407−418.
(76) Okae, I., and Iwakura, Y. (2010) Neural tube defects and impaired neural progenitor cell proliferation in Gβ1-deficient mice. *Dev. Dyn. 239*, 1089−1101.
(77) Schwindinger, W. F., Borrell, B. M., Waldman, L. C., and Robishaw, J. D. (2009) Mice lacking the G protein γ_3-subunit show resistance to opioids and diet induced obesity. *Am. J. Physiol. 297*, R1494−R1502.
(78) Dippel, E., Kalkbrenner, F., Wittig, B., and Schultz, G. (1996) A heterotrimeric G protein complex couples the muscarinic m1 receptor to phospholipase C-β. *Proc. Natl. Acad. Sci. U.S.A. 93*, 1391−1396.
(79) Mahmoud, S., Yun, J. K., and Ruiz-Velasco, V. (2012) Gβ_2 and Gβ_4 participate in the opioid and adrenergic receptor-mediated Ca^{2+} channel modulation in rat sympathetic neurons. *J. Physiol. 590*, 4673−4689.
(80) Zachariou, V., Georgescu, D., Sanchez, N., Rahman, Z., DeLeone, R., Berton, O., Neve, R. L., Sim-Selley, L. J., Selley, D. E., Gold, S. J., and Nestler, E. J. (2003) Essential role for RGS9 in opiate action. *J. Neurosci. 29*, 13656−13661.
(81) López-Fando, A., Rodríguez-Muñoz, M., Sánchez-Blázquez, P., and Garzón, J. (2005) Expression of neural RGS-R7 and Gβ_5 proteins in response to acute and chronic morphine. *Neuropsychopharmacology 30*, 99−110.
(82) Anderson, G. R., Cao, Y., Davidson, S., Truong, H. V., Pravetoni, M., Thomas, M. J., Wickman, K., Giesler, G. J., and Martemyanov, K. A. (2010) R7BP complexes with RGS9-2 and RGS7 in the striatum differentially control motor learning and locomotor responses to cocaine. *Neuropsychopharmacology 35*, 1040−1050.
(83) Psifogeorgou, K., Terzi, D., Papachatzaki, M. M., Varidaki, A., Ferguson, D., Gold, S. J., and Zhachariou, V. (2011) A unique role of RGS9-2 in the striatum as a positive or negative regulator of opiate analgesia. *J. Neurosci. 31* (15), 5617−5624.
(84) Mashuho, I., Xie, K., and Martemyanov, K. A. (2013) Macromolecular composition dictates receptor and G protein selectivity of regulator of G protein signaling (RGS) 7 and 9-2 protein complexes in living cells. *J. Biol. Chem. 288*, 25129−25142.
(85) Gold, S. J., Ni, Y. G., Dohlman, H. G., and Nestler, E. J. (1997) Regulators of G protein signaling (RGS) proteins: Region-specific expression of nine subtypes in rat brain. *J. Neurosci. 17*, 8024−8037.
(86) Anderson, G. R., Lujan, R., Semenov, A., Pravetoni, M., Posokhova, E. N., Song, J. H., Uversky, V., Chen, C.-K., Wickman, K., and Martemyanov, K. R. (2007) Expression and localization of RGS9-2/Gβ_5/R7BP complex *in vivo* is set by dynamic control of its constitutive degradation by cellular cysteine proteases. *J. Neurosci. 27* (51), 14117−14127.
(87) Anderson, G. R., Lujan, R., and Martemyanov, K. R. (2009) Changes in striatal signaling induce remodeling of RGS complexes containing Gβ_5 and R7BP subunits. *Mol. Cell. Biol. 29* (11), 3033−3044.
(88) Song, J. H., Waataja, J. J., and Martemyanov, K. A. (2006) Subcellular targeting of RGS9-2 is controlled by multiple molecular determinants on its membrane anchor, R7BP. *J. Biol. Chem. 281*, 15361−15369.
(89) Cook, L. A., Schey, K. L., Wilcox, M. D., Dingus, J., Ettling, R., Nelson, T., Knapp, D. R., and Hildebrandt, J. D. (2006) Proteomic analysis of bovine G protein γ subunit processing heterogeneity. *Mol. Cell. Proteomics 5* (4), 671−685.
(90) Kelley, A. E., Bakshi, V. P., Haber, S. N., Steininger, T. L., Will, M. J., and Zhang, M. (2002) Opioid modulation of taste hedonics within the ventral striatum. *Physiol. Behav. 76* (3), 365−377.
(91) Ward, H. G., Nicklous, D. M., Aloyo, V. J., and Simansky, K. J. (2006) Mu-opioid receptor cellular function in the nucleus accumbens is essential for hedonically driven eating. *Eur. J. Neurosci. 23*, 1605−1613.
(92) Brudege, J. M., and Williams, J. T. (2002) Differential modulation of nucleus accumbens synapses. *J. Neurophysiol. 88* (1), 142−151.
(93) Schwindinger, W. F., Betz, K. S., Giger, K. E., Sabol, A., Bronson, S. K., and Robishaw, J. D. (2003) Loss of G protein γ_7 alters behavior and reduces striatal α_{olf} level and cAMP production. *J. Biol. Chem. 278* (8), 6575−6579.
(94) Schwindinger, W. F., Mihalcik, L. J. M., Giger, K. E., Betz, K. S., Stauffer, A. M., Linden, J., Herve, D., and Robishaw, J. D. (2010) Adenosine A_{2A} receptor signaling and G_{olf} assembly show a specific requirement for the γ_7 subtype in the striatum. *J. Biol. Chem. 285* (39), 29787−29796.
(95) Watson, J. B., Coulter, P. M., II, Marguiles, J. E., de Lecea, L., Danielson, P. E., Erlander, M. G., and Sutcliffe, J. G. (1994) G-protein γ7 subunit is selectively expressed in medium-sized neurons and dendrites of the rat neostriatum. *J. Neurosci. Res. 39* (1), 108−116.
(96) Caillé, I., Dumartin, B., and Bloch, B. (1996) Ultrastructural localization of D1 dopamine reactivity in rat striatonigral neurons and its relation with dopamine innervation. *Brain Res. 730*, 17−31.
(97) Hettinger, B. D., Lee, A., Linden, J., and Rosin, D. L. (2001) Ultrastructural localization of adenosine A_{2A} receptors suggests multiple cellular sites for modulation of GABAergic neurons in rat striatum. *J. Comp. Neurol. 431*, 331−346.
(98) Kalkbrenner, F., Degtiar, V. E., Schenker, M., Brendal, S., Zobel, A., Heschler, J., Wittig, B., and Schultz, G. (1995) Subunit composition of G_o proteins functionally coupling galanin receptors to voltage-gated calcium channels. *EMBO J. 14* (19), 4728−4737.
(99) Hosohata, K., Logan, J. K., Varga, E., Burkey, T. H., Vanderah, T. W., Porreca, F., Hruby, V. J., Roeske, W. R., and Yamamura, H. I. (2000) The role of the G protein γ_2 subunit in opioid antinociception in mice. *Eur. J. Pharmacol. 392*, R9−R11.
(100) Varga, E. V., Hosohata, K., Borys, D., Navratilova, E., Nylen, A., Vanderah, T. W., Porreca, F., Roeske, W. R., and Yamamura, H. I. (2005) Antinociception depends on the presence of G protein γ_2-subunits in brain. *Eur. J. Pharmacol. 508*, 93−98.
(101) Mitsukawa, K., Lu, X., and Bartfai, T. (2010) Galanin, galanin receptors, and drug targets. *Experientia, Suppl. 102*, 7−23.
(102) Kitchen, I., Slowe, S. J., Matthes, H., and Kieffer, B. (1997) Quantitative autoradiographic mapping of mu-, delta-, and kappa-opioid receptors in knockout mice lacking the mu-opioid receptor gene. *Brain Res. 778*, 73−88.
(103) Slowe, S. J., Simonin, F., Kieffer, B., and Kitchen, I. (1999) Quantitative autoradiography of mu-, delta-, and kappa-opioid receptors in kappa-opioid receptor knockout mice. *Brain Res. 818*, 335−345.
(104) Goody, R. J., Oakley, S. M., Filliol, D., Kieffer, B., and Kitchen, I. (2002) Quantitative autoradiographic mapping of opioid receptors in the brain of delta opioid receptor gene knockout mice. *Brain Res. 945*, 9−19.
(105) Huang, L., Shanker, Y. G., Dubauskaite, J., Zheng, J. Z., Yan, W., Rosenzweig, S., Spielman, A. I., Max, M., and Margolskee, R. F. (1999) Gγ13 colocalizes with gustducin in taste receptor cells and mediates IP3 responses to bitter denatonium. *Nat. Neurosci. 2*, 1055−1062.
(106) Blake, B. L., Wing, M. R., Zhou, J. Y., Lei, Q., Hillmann, J. R., Behe, C. I., Morris, R. A., Harden, T. K., Bayliss, D. A., Miller, R. J., and Siderovski, D. P. (2001) Gβ association and effector interaction selectivities of the divergent Gγ subunit $G\gamma_{13}$. *J. Biol. Chem. 276* (52), 49267−49274.
(107) Fujino, A., Pieretti-Vanmarcke, R., Wong, A., Donahoe, P. K., and Arango, N. A. (2007) Sexual dimorphism of G-protein subunit *Gng13* expression in the cortical region of the developing mouse ovary. *Dev. Dyn. 236*, 1991−1996.
(108) Li, Z., Benard, O., and Margolskee, R. F. (2006) $G\gamma_{13}$ interacts with PDZ domain containing proteins. *J. Biol. Chem. 81* (16), 11066−11073.

(109) Huang, Q., Zhou, D., Chase, K., Gusella, J. F., Aronin, N., and DiFiglia, M. (1992) Immunohistochemical localization of the D1 dopamine receptor in rat brain reveals its axonal transport, pre- and postsynaptic localization, and prevalence in the basal ganglia, limbic system, and thalamic reticular neurons. *Proc. Natl. Acad. Sci. U.S.A. 89*, 11988−11992.
(110) Kreitzer, A. C., and Malenka, R. C. (2008) Striatal plasticity and basal ganglia circuit function. *Neuron 60* (4), 543−554.
(111) Prange-Kiel, J., and Rune, G. M. (2006) Direct and indirect effects of estrogen on rat hippocampus. *Neuroscience 138* (3), 765−772.
(112) Leranth, C., and Hajszan, T. (2007) Extrinsic afferent systems to the dentate gyrus. *Prog. Brain Res. 163*, 63−84.
(113) Harley, C. (2007) Norepinephrine and the dentate gyrus. *Prog. Brain Res. 163*, 299−318.
(114) Schliebs, R., and Arendt, T. (2011) The cholinergic system in aging and neuronal degeneration. *Behav. Brain Res. 221* (2), 555−563.
(115) Cesa, R., and Strata, P. (2009) Axonal competition in the synaptic wiring of the cerebellar cortex during development and in the mature cerebellum. *Neurosci. Res. 163*, 299−318.